Journal of Inorganic and General Chemistry
ZAAC
Zeitschrift für anorganische und allgemeine Chemie
DOI: 10.1002/zaac.202000249
ARTICLE

Phosphino-Stibine Ligands for the Synthesis of Heterometallic Complexes

Martin Piesch,[a] Francois P. Gabbaï,[b] and Manfred Scheer*[a]

Dedicated to Professor Thomas Klapötke on the Occasion of his 60th Birthday

Abstract. The phosphino-stibine ligands (o-$PPh_2C_6H_4)_2SbR$ [R = o-$PPh_2C_6H_4$ (**L1**), Ph (**L2**), Cl (**L3**)] were incorporated into tungsten and molybdenum carbonyl complexes leading to the formation of *cis*-[$W(CO)_4${(o-$PPh_2C_6H_4)_2SbR$}] [R = o-$PPh_2C_6H_4$ (**1**), Ph (**2**), Cl (**3**)], *fac*-[$W(CO)_3${(o-$PPh_2C_6H_4)_3Sb$}] (**4**), *fac*-[$W(CO)_3${(o-$PPh_2C_6H_4)_2SbCl$}] (**5**), *fac*-[($W(CO)_3${(o-$PPh_2C_6H_4)_2Sb$})$_2$] (**6**), *fac*-[$Mo(CO)_3${(o-$PPh_2C_6H_4)_2SbR$}] [R = o-$PPh_2C_6H_4$ (**7**), Ph (**8**), Cl (**9**)]. Compounds **1** and **4** were allowed to react with MX salts with M = Cu, Ag, Au and X = Cl^-, $[PF_6]^-$, respectively. These reactions yielded *cis*-[$W(CO)_4${(o-$PPh_2C_6H_4)_3Sb$}{MCl}] [M = Cu (**10**), Ag (**11**)], *cis*-[$W(CO)_4${(o-$PPh_2C_6H_4)_2Sb$}{AuCl(o-$PPh_2C_6H_4$)}{AuCl}] (**12**) *cis*-[($W(CO)_4${(o-$PPh_2C_6H_4)_2Sb$})$_2$AuCl] (**13**), *cis*-[$W(CO)_3$(μ-CO){(o-$PPh_2C_6H_4)_3Sb$}{Cu}][PF_6] (**14**), *cis*-[$W(CO)_4${(o-$PPh_2C_6H_4)_3Sb$}{AgMeCN}][PF_6] (**15**), *cis*-[$W(CO)_4${(o-$PPh_2C_6H_4)_3Sb$}{Au}][PF_6] (**16**) *cis*-[$W(CO)_2$(μ-CO){(o-$PPh_2C_6H_4)_3Sb$}{Cu_2(μ-Cl)$_2$}] (**17**), *fac*-[$W(CO)_3${(o-$PPh_2C_6H_4)_3Sb$}{AuCl}] (**18**), and *fac*-[$W(CO)_2$(μ-CO){(o-$PPh_2C_6H_4)_3Sb$}{ML}][PF_6] [M = Cu, L = MeCN (**19**), M = Ag, L = MeCN (**20**), M = Au (**21**)]. Complexes **10**–**21** all show metal-metal distances below the sum of the corresponding van der Waals radii. The proximity of the two metal centers is especially significant in **19**–**21**, indicating the presence of metal-metal bonding.

Introduction

When compared to the ubiquitous phosphine ligands, stibines display markedly reduced donor properties because of the higher s character and the poor availability of the pnictogen-centered lone pair.[1–3] One strategy to favor the coordination of stibines to metals is based on the incorporation of the antimony atom in a polydentate scaffold where ancillary ligands such as phosphines promote metal complexation. A well-known class of such ligands are phosphino-stibine ligands of the type (o-$PR_2C_6H_4)_3Sb$.[4] These ligands are soft σ-donors and can undergo an antimony-centered two-electron oxidation, providing control over the ligative characteristics of the antimony center. These ligands have been incorporated into several late transition metal complexes.[2,3] The phenyl-substituted ligand can be combined with (tht)AuCl to yield [(o-$PPh_2C_6H_4)_3SbAuCl$] (**A**) in which the gold center is coordinated by the antimony atom and two phosphine arms (see Figure 1). Complex **A** can be oxidized using $PhICl_2$ to give [(o-$PPh_2C_6H_4)_3SbCl_2AuCl$] (**B**) (see Figure 1). In this reaction an umpolung of the Au–Sb interaction takes place. In **A** a lone pair of Sb donates to Au, while in **B** Au donates to Sb.[5] The isopropyl-substituted ligand can be reacted with CuCl and AgCl, respectively, to form the trinuclear cluster [(o-PiPr$_2C_6H_4)_3SbM_3$(μ-Cl)$_3$] (M = Cu, Ag) (**C**), where each metal atom is coordinated by the antimony atom and one phosphine arm of the ligand while three chlorine atoms are bridging all Cu and Ag atoms, respectively (see Figure 1).[6]

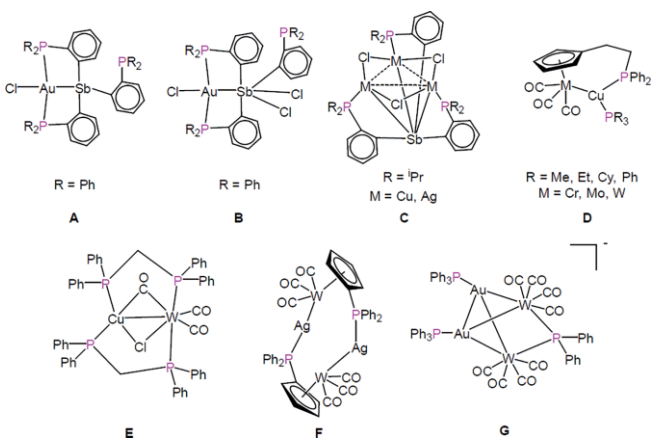

Figure 1. Selected complexes with polydentate phosphino stibine ligands and heterometallic complexes based on group six and coinage metals.

Phosphine-based multidentate ligands, that do not contain an antimony atom, have also been used to support the formation of multi-metallic systems with short metal–metal contacts.

* Prof. Dr. M. Scheer
E-Mail: Manfred.Scheer@ur.de
https://www.uni-regensburg.de/chemie-pharmazie/anorganische-chemie-scheer/
[a] Institut für Anorganische Chemie
Universität Regensburg
93040 Regensburg, Germany
[b] Department of Chemistry
Texas A&M University
College Station, TX 77843–3255, USA
Supporting information for this article is available on the WWW under **http://dx.doi.org/10.1002/zaac.202000249** or from the author.

This approach is illustrated by efforts dealing with the synthesis of complexes containing group six and coinage metals as in the case of complexes of type **D**, of general formula $[(C_5H_4(CH_2)_2PPh_2)M(CO)_3Cu(PR_3)]$ (M = Cr, Mo, W).[7] In these complexes, a dangling diphenylphosphine side arm forces the copper atom into the coordination sphere of the group 6 metal. Diphosphine ligands such as bis(diphenylphosphanyl)methane (dppm) can be used to also support short metal-metal contacts as in the case of $[(CO)_2W(\mu\text{-}Ph_2PCH_2PPh_2)_2(\mu\text{-}CO)(\mu\text{-}Cl)Cu]$ (**E**) which also features bridging CO and Cl^- ligands.[8] Similar strategies have afforded $[(CO)_3W(\mu\text{-}C_5H_4PPh_2)Ag]_2$ (**F**)[9] and $[NEt_4][(\mu\text{-}PPh_2)(\mu\text{-}(Ph_3PAu)_2)W_2(CO)_8]$ (**G**),[10] a family of complexes that also feature group 6 metals with a coinage metals in their immediate proximity. The structures of complexes **A**–**G** are depicted in Figure 1.

In this study, we have explored the use of three multidentate phosphino-stibine ligands of general formula $(o\text{-}PPh_2C_6H_4)_2SbR$ with R = o-$PPh_2C_6H_4$ (**L1**), Ph (**L2**), Cl (**L3**) as platforms for the formation of complexes featuring a group six metal carbonyl in close interaction with a coinage metal ion. The strategy developed for this study is based on two steps. The first step consists of the coordination to the group 6 metal by reaction with $[W(CO)_4(nbd)]$ (nbd = 2,5-norbonadiene), $[W(CO)_3(cht)]$ (cht = 1,3,5-cycloheptatriene) and $[Mo(CO)_3(cht)]$, respectively. In the second step, the resulting complexes are allowed to react with coinage metal salts.

Results and Discussion

Allowing ligands **L1**–**L3** to react with $[W(CO)_4(nbd)]$ in boiling thf overnight leads to the formation of *cis*-$[W(CO)_4\{(o\text{-}PPh_2C_6H_4)_2SbR\}]$ [R = o-$PPh_2C_6H_4$ (**1**), Ph (**2**), Cl (**3**)] in crystalline yields of 72, 65 and 68 % [see Equation (1)]. Compounds **1**–**3** can be obtained as bright yellow solids.

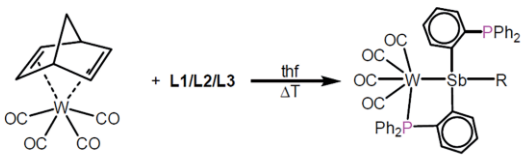

(1)

R = o-$PPh_2C_6H_4$ (**1**, 72 %)
R = Ph (**2**, 65 %)
R = Cl (**3**, 68 %)

Crystals suitable for single-crystal X-ray structure analysis were obtained from concentrated solutions in thf (**1**), CH_2Cl_2 (**2**), or dimethoxyethane (**3**) layered with pentane (**1**) or hexane (**2**, **3**). The structures of these complexes (Figure 2) reveal that one phosphine group and the antimony atom are coordinated to the $\{W(CO)_4\}$ fragment, while the other phosphine substituents remain unengaged. In each of the $^{31}P\{^1H\}$ NMR spectra, two singlets at δ = 56.9 and –5.0 ([D_8]thf, **1**), 54.8 and –4.7 (CD_2Cl_2, **2**), 56.7 and –12.2 ppm ([D_8]thf, **3**) can be observed, while the downfield shifted signals show additional tungsten satellites with $^1J_{PW}$ coupling constants in the range of 223 and 229 Hz. It is notable, that the signal for the free phosphine group in **3** is shifted upfield when compared to those in **1** and **2**. A possible explanation is a weak interaction between Sb1 and P2, as indicated by a Sb···P distance of 3.1404(7) Å. This distance is ~0.34 Å shorter than those observed in **1** (average 3.4833 Å) and is ca. 0.18 Å shorter than those observed in **2** (average 3.3243 Å).

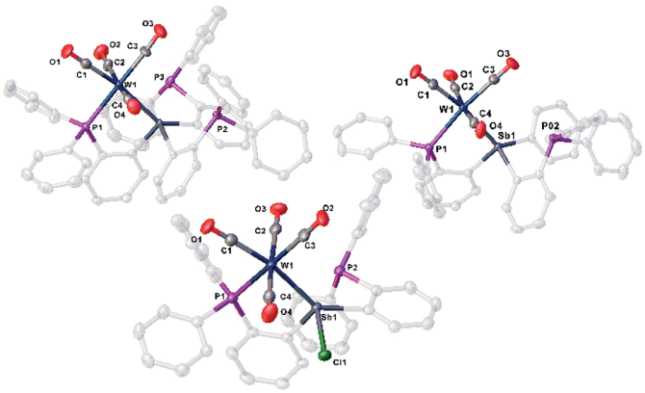

Figure 2. Molecular structures of **1** (top, left), **2** (top, right) and **3** (bottom) in the solid state. Thermal ellipsoids are shown at 50 % probability level. Hydrogen atoms and solvent molecules are omitted for clarity.

Reaction of **L1** with $[W(CO)_3(cht)]$ (cht = 1,3,5-cycloheptatriene) in boiling thf overnight leads to the formation of *fac*-$[W(CO)_3\{(o\text{-}PPh_2C_6H_4)_3Sb\}]$ (**4**) [see [Equation (2<ffr2" pos="x11>)]. Compound **4** was isolated as a dark yellow crystalline solid in 53 % yield. Alternatively, **4** could be generated by irradiation of a solution of **1** in thf for several hours or by reflux of **1** in decalin for 12 h. In both cases, purification of **4** necessitated column chromatography. It follows that accessing **4** starting from **1** is less efficient than starting from **L1** with $[W(CO)_3(cht)]$. The isolated yields were 27 % and 11 %, for the photolysis and thermolysis of **1**, respectively.

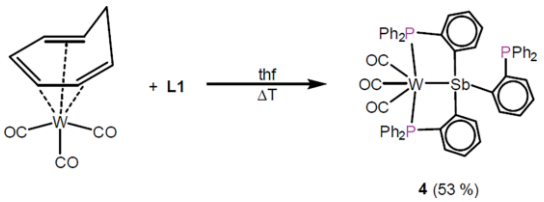

(2)

4 (53 %)

Crystals suitable for single-crystal X-ray structure analysis can be obtained from a concentrated solution in CH_2Cl_2 layered with hexane. The structure of **4** (Figure 3) reveals that

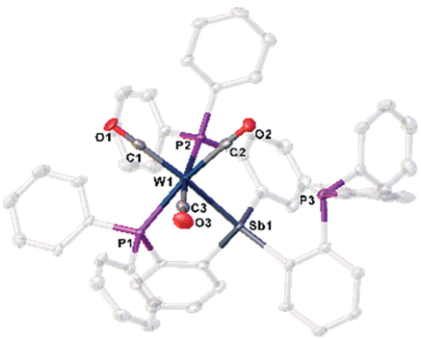

Figure 3. Molecular structure of **4** in the solid state. Thermal ellipsoids are shown at 50 % probability level. Hydrogen atoms are omitted for clarity.

two phosphine arms and the antimony atom are coordinated to the $\{W(CO)_3\}$ fragment, while one phosphine substituent remains free. In the $^{31}P\{^1H\}$ NMR spectrum in $[D_8]$thf, two singlets at δ = 57.8 and –4.7 can be observed, while the downfield signal show additional tungsten satellites with $^1J_{PW}$ coupling constant of 220 Hz. When *cis*-$[W(CO)_4\{(o\text{-}PPh_2C_6H_4)_2SbCl\}]$ (**3**) is irradiated with UV light, *fac*-$[W(CO)_3\{(o\text{-}PPh_2C_6H_4)_2SbCl\}]$ (**5**) and *fac*-$[(W(CO)_3\{(o\text{-}PPh_2C_6H_4)_2Sb\})_2]$ (**6**) can be isolated after column chromatography as orange solids in low yields [see Equation (3)].

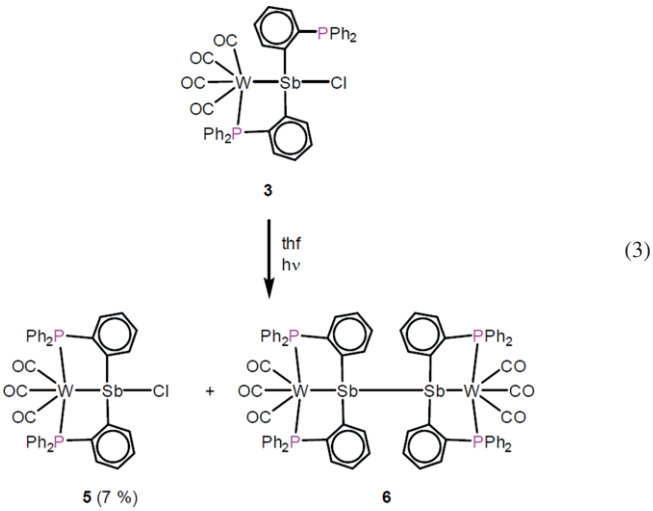

(3)

Crystals suitable for single-crystal X-ray structure analysis can be obtained from concentrated solutions in thf (for **5**) or CH_2Cl_2 (for **6**) layered with pentane (for **5**) or hexane (for **6**). The structures of these complexes, which are depicted in Figure 4, confirm the removal of a CO ligand upon irradiation. The structure of **5** shows that the $\{W(CO)_3\}$ fragment is coordinated by two phosphine groups and the antimony atom. The structure of **6** indicates the existence of a dimer consisting of two $\{W(CO)_3\{(o\text{-}PPh_2C_6H_4)_2Sb\}$ fragments connected by an Sb–Sb bond. Compound **6** can be regarded as a reduction product of **5**. Formation of **6** may be assisted by oxidative decomposition of the ligand or of the group 6 metal fragment. Such processes, which must be involved to explain the reduction of the antimony atom, are also consistent with the low isolated yields. The $^{31}P\{^1H\}$ NMR spectra of **5** in CD_2Cl_2 and **6** in

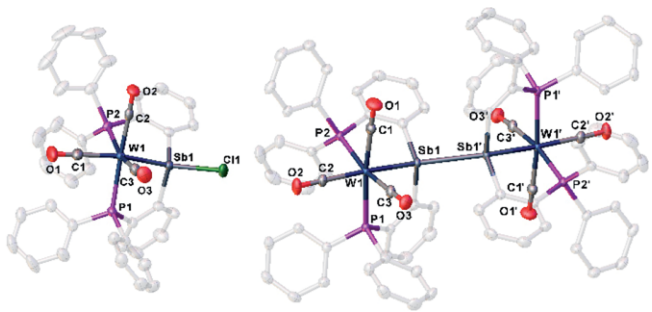

Figure 4. Molecular structures of **5** (left) and **6** (right) in solid state. Thermal ellipsoids are shown at 50 % probability level. Hydrogen atoms and solvent molecules are omitted for clarity.

$[D_8]$thf display a singlet at δ = 52.4 for **5** and 57.1 ppm for **6**. Both signals show a $^1J_{PW}$ coupling constant of 212 Hz (**5**) and 104 Hz (**6**), respectively.

The reaction of ligands **L1**–**L3** with $[Mo(CO)_3(cht)]$ (cht = 1,3,5-cycloheptatriene) in boiling thf was also investigated. These reactions afforded complexes **7**–**9** of general formula *fac*-$[Mo(CO)_3\{(o\text{-}PPh_2C_6H_4)_2SbR\}]$ with R = $(o\text{-}PPh_2C_6H_4)$ for **7**, R = Ph for **8**, and R = Cl for **9**. These complexes were obtained as crystalline solids in yields of 57, 47 and 25 %, respectively [Equation (4)]. Complexes **7** and **8** display a yellow color while compound **9** is orange.

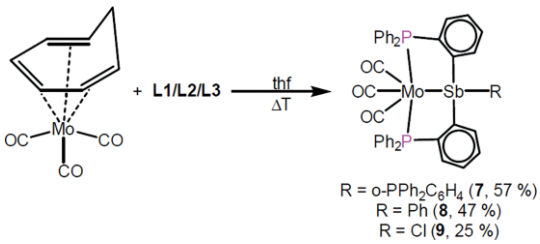

(4)

Crystals suitable for single-crystal X-ray structure analysis were obtained from concentrated solutions in CH_2Cl_2 (**7**,**9**) or dimethoxyethane (**8**) layered with hexane. The solid-state structures of these complexes are shown in Figure 5. The structure reveals that two phosphine ligands and the antimony atom are coordinated to the $\{Mo(CO)_3\}$ fragment, while the third substituent remains free. In the $^{31}P\{^1H\}$ NMR spectrum of **7** in CD_2Cl_2, two singlets at δ = 71.2 and –6.3 ppm can be detected. In the $^{31}P\{^1H\}$ spectra of **8** and **9** in $[D_8]$thf one singlet at δ = 73.4 (**8**) and 66.6 ppm (**9**) can be observed.

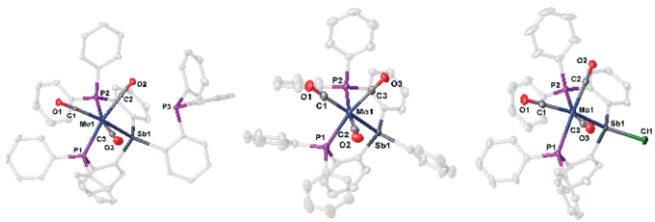

Figure 5. Molecular structures of **7** (left), **8** (middle) and **9** (right) in solid state. Thermal ellipsoids are shown at 50 % probability level. Hydrogen atoms and solvent molecules are omitted for clarity.

With these metal carbonyl complexes in hand and in particular those containing free phosphine ligands, we decided to investigate their reactions with coinage metal salts. The reaction of *cis*-$[W(CO)_4\{(o\text{-}PPh_2C_6H_4)_3Sb\}]$ (**1**) with one equivalent of CuCl and AgCl (the latter under ultrasonic conditions), respectively leads to the formation of *cis*-$[W(CO)_4\{(o\text{-}PPh_2C_6H_4)_3Sb\}\{MCl\}]$ [M = Cu (**10**), Ag (**11**)] isolated as crystalline solids in yields of 78 and 35 %, respectively (Scheme 1). Crystals suitable for single-crystal X-ray structure analysis were obtained after a few days upon layering concentrated solutions of the complexes in CH_2Cl_2 with hexane at room temperature. The structures of **10** and **11** in the solid state (Figure 6) show that the metal halides have been incorporated in the binding pocket of **1**. The Cu and Ag ions, respectively, are coordinated by the two phosphine side groups (P2 and P3) and the central Sb atom of the ligand framework. Due

to the geometry of the ligand, the Cu and Ag atoms are brought into proximity of the {$W(CO)_4$} fragment with W1–Cu1 and W1–Ag1 distances of 3.2383(5) Å and 3.1893(3)/3.3342(3) Å, respectively.

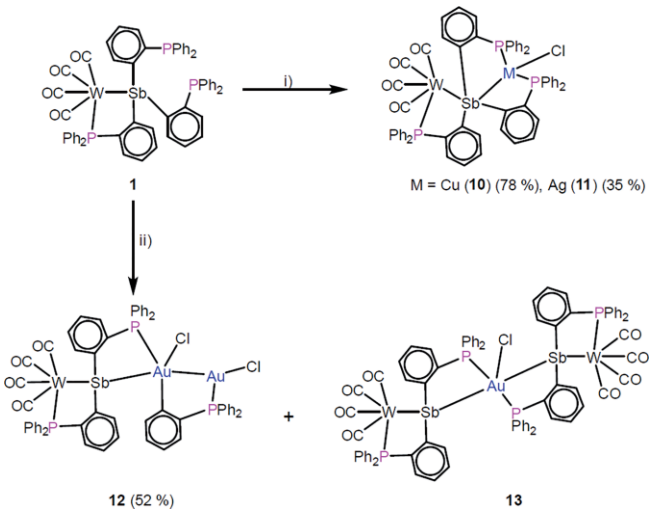

Scheme 1. Reaction of **1** with (i) CuCl or AgCl and (ii) (tht)AuCl in CH_2Cl_2 at room temperature.

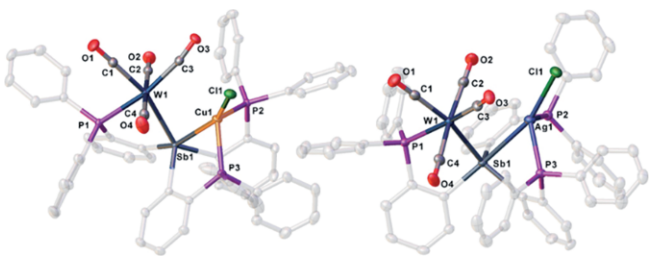

Figure 6. Molecular structures in solid state of **10** (left) and **11** (right). Thermal ellipsoids are drawn with 50 % probability level. Solvent molecules and hydrogen atoms are omitted for clarity.

The crystal structure of **11** shows two independent molecules with different W–Ag distances [3.1893(3) and 3.3342(3) Å] probably due to packing effects. These distances are below the sum of van der Waals radii [Σ_{vdW} (W–Cu) = 4.95 Å, Σ_{vdW} (W–Ag) = 5.10 Å].[11] Yet, calculated Wiberg Bond Indices (WBIs, BP86/def2-TZVP level of theory) of 0.03 for each complex suggest that if bonding is present, it much be very weak.

Allowing **1** to react with two equivalents of (tht)AuCl afford a 52 % yield of *cis*-[$W(CO)_4${(o-$PPh_2C_6H_4)_2Sb$}{AuCl(o-$PPh_2C_6H_4$)}{AuCl}] (**12**) as a crystalline solid. This reaction also afford traces of *cis*-[($W(CO)_4${(o-$PPh_2C_6H_4)_2Sb$})$_2$AuCl] (**13**) (Scheme 1). Using a 1:1 stoichiometry, the reaction leads to a mixture of **1** and **12** (1:1), according to $^{31}P\{^1H\}$ NMR spectroscopy. Crystals of **12** suitable for single-crystal X-ray structure analysis were obtained from a concentrated solution in o-$C_6H_4F_2$ layered with hexane at room temperature. Very few single crystals of **13** could be obtained from this crystallization setup after several weeks. The structure of **12** in the solid state (Figure 7, left) shows that one {AuCl} fragment has been inserted in an antimony–carbon bond of the ligand. This Au1 atom is coordinated by one phosphine group (P2) which is still connected to the central Sb atom of the ligand framework. The third phosphine arm which is now connected to Au1 via the phenylene backbone, engages a second gold atom (Au2) which forms an aurophilic interaction as indicated by its proximity to Au1 (Au1–Au2 distance of 3.1302(2) Å]. Compound **13** is probably a decomposition product of **12**. The structure of **13** in the solid state (Figure 7, right) reveals a complex where a central {AuCl} unit is coordinated by two ($W(CO)_4${(o-$PPh_2C_6H_4)_2Sb$}) fragments which have both lost one coordinating phosphine arm.

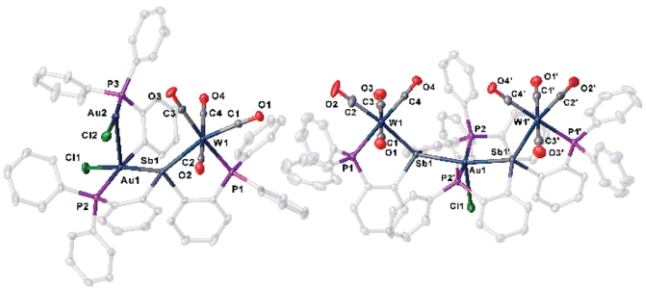

Figure 7. Molecular structure in the solid state of **12** (left) and **13** (right). Thermal ellipsoids are drawn with 50 % probability level. Solvent molecules and hydrogen atoms are omitted for clarity.

To increase the strength of the interaction between the coinage metals and tungsten, we decided to replace the chloride counter anion with the weakly coordinating hexafluorophosphate anion. We posited that this simple swap would leave the coinage metal more exposed and thus more susceptible to interacting with the group 6 metal. The reagents used to test this idea include [$Cu(MeCN)_4$][PF_6] and Ag[PF_6]. In the case of gold, Au[PF_6], which is not a stable and isolable salt, was generated *in situ* in the presence of **1**. The reaction of **1** with [$Cu(MeCN)_4$][PF_6], Ag[PF_6] and in situ generated "Au[PF_6]" gives *cis*-[$W(CO)_3$(μ-CO){(o-$PPh_2C_6H_4)_3Sb$}{Cu}][PF_6] (**14**), *cis*-[$W(CO)_4${(o-$PPh_2C_6H_4)_3Sb$}{AgMeCN}][PF_6] (**15**) and *cis*-[$W(CO)_4${(o-$PPh_2C_6H_4)_3Sb$}{Au}][PF_6] (**16**) as crystalline solids in yields of 70, 69 and 69 %, respectively (Scheme 2).

Crystals suitable for single-crystal X-ray structure analyses can be obtained from concentrated solutions in o-$C_6H_4F_2$ (for **14**) or CH_2Cl_2 (for **15** and **16**) layered with pentane (for **14**) or hexane (for **15** and **16**) at room temperature.

The structures of **14**–**16** in the solid state (Figure 8) reveal that the coinage metal ions have been incorporated in the binding pocket of **1** and are coordinated by two phosphine units. For **14** an additional coordination of one carbonyl ligand is observed as indicated by the C1–Cu1 distance of 2.407(7) Å, comparable with values found in [$CpW(CO)(\mu$-$CO)_2Cu(PPh_3)_2$].[12] The bridging binding mode of the carbonyl ligand in **14** is also confirmed by a band in the IR spectrum at 1826 cm^{-1} which is shifted to lower wavenumbers, compared to the other bands of **14** at 2032, 1943 and 1928 cm^{-1}. The Ag atom in **15** is saturated by an acetonitrile ligand. The coinage metal-tungsten distances amount to 2.8645(11) Å in **14**, 3.2290(4) Å in **15** and 3.14079(16) Å in **16**. Although all W–M distances are below the sum of the van

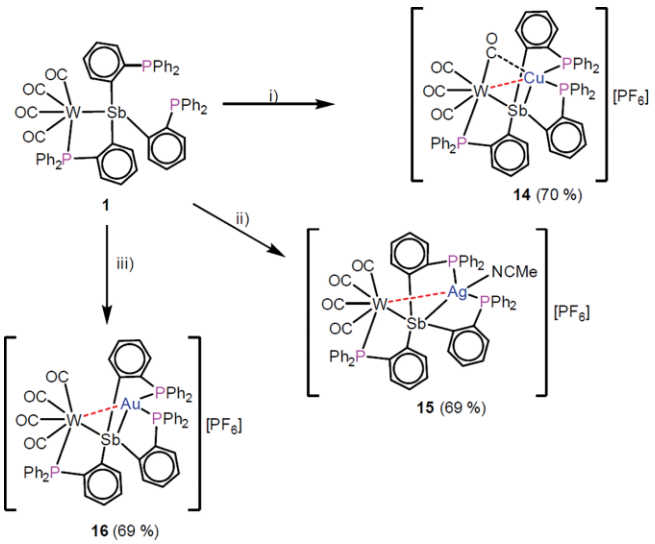

Scheme 2. Reaction of **1** with (i) $[Cu(MeCN)_4][PF_6]$, (ii)$Ag[PF_6]$, and (iii) $Tl[PF_6]$ and (tht)AuCl in CH_2Cl_2 at room temperature.

der Waals radii [Σ_{vdW} (W–Cu) 4.95, (W–Ag) = 5.10, (W–Au) 4.89 Å],[11] no significant interactions are present. The absence of strong interaction is supported by WBI values of 0.06 for **14**, 0.04 for **15**, and 0.03 for **16**.

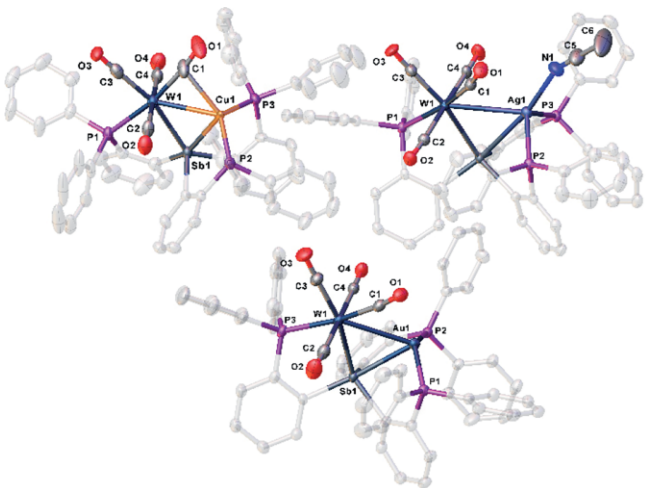

Figure 8. Molecular structures of the cations in **14** (top left), **15** (top right) and **16** (bottom) in the solid state. Thermal ellipsoids are drawn with 50 % probability level. Hydrogen atoms are omitted for clarity.

An analog reactivity study was performed for *fac*-$[W(CO)_3\{(o\text{-}PPh_2C_6H_4)_3Sb\}]$ (**4**), which has only one free phosphine group while **1** has two. The reaction of **4** with CuCl and (tht)AuCl yields *cis*-$[W(CO)_2(\mu\text{-}CO)\{(o\text{-}PPh_2C_6H_4)_3Sb\}\{Cu_2(\mu\text{-}Cl)_2\}]$ (**17**) and *fac*-$[W(CO)_3\{(o\text{-}PPh_2C_6H_4)_3Sb\}\{AuCl\}]$ (**18**) as crystalline solids in yields of 88 and 40 %, respectively (Scheme 3). Crystals of **17** and **18** suitable for single crystals X-ray structure analysis were obtained from concentrated solutions in CH_2Cl_2 layered with hexane at room temperature.

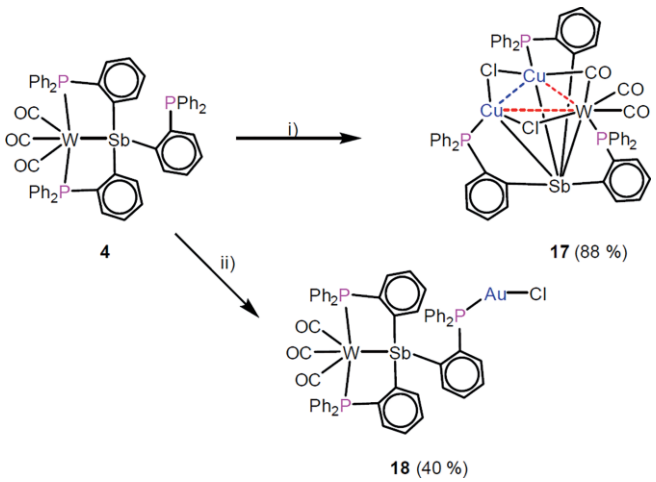

Scheme 3. Reaction of **4** with (i) CuCl and (ii) (tht)AuCl in CH_2Cl_2 at room temperature.

The structure of **17** in the solid state (Figure 9, left) reveals a trinuclear complex with a central three membered WCu_2 ring motif. The edges of the metallacycle are bridged by two chlorine atoms (W1–Cu1 and Cu1–Cu2) and one carbonyl ligand (W1–Cu2). Due to the asymmetry of the complex, two different W–Cu distances are present [W1–Cu1 3.0849(11) and W1–Cu2 2.8359(11) Å]. The Cu1–Cu2 distance amounts to 2.6826(14) Å. All M–M distances are below the sum of van der Waals radii [Σ_{vdW} (W–Cu) 4.95, (Cu–Cu) 4.76 Å] and only very weak interactions are present based on the WBI values of 0.05, 0.06, and 0.03 for the W1–Cu1 W1–Cu2, and Cu1–Cu2 contacts, respectively.

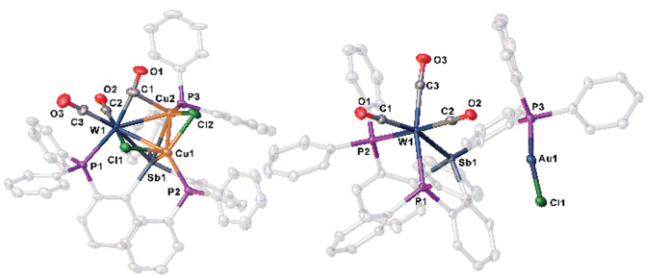

Figure 9. Molecular structures of **17** (left) and **18** (right) in the solid state. Thermal ellipsoids are drawn with 50 % probability level. Solvent molecules and hydrogen atoms are omitted for clarity.

The coordination of only one equivalent of CuCl to **4** was not successful. The structure of the gold complex **18** in the solid state (Figure 5, right) shows that {AuCl} was coordinated by the last free phosphine group and directed away from the tungsten atom. The Au atom is coordinated almost linearly as indicated by the P–Au–Cl angle of 171.02(5)°. To get a closer M···W contact the coinage metal salts containing the weakly coordinating $[PF_6]^-$ anion were used. The reaction of **4** with $[Cu(MeCN)_4][PF_6]$, $Ag[PF_6]$ and *in situ* generated "$Au[PF_6]$" yields *fac*-$[W(CO)_2(\mu\text{-}CO)\ \{(o\text{-}PPh_2C_6H_4)_3Sb\}\{ML\}][PF_6]$ [M = Cu, L = MeCN (**19**), M = Ag, L = MeCN (**20**), M = Au (**21**)] as crystalline solids in yields of 96, 70 and 66 %, respectively (Scheme 4).

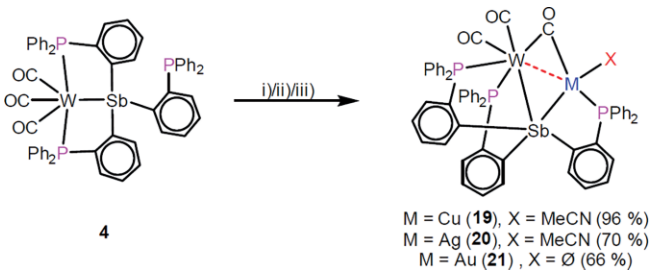

Scheme 4. Reaction of **4** with (i) $[Cu(MeCN)_4][PF_6]$, (ii) $Ag[PF_6]$, and (iii) (tht)AuCl and $Tl[PF_6]$ in CH_2Cl_2 at room temperature.

Crystals suitable for X-ray single crystal structure analysis can be obtained from concentrated solutions in CH_2Cl_2 layered with hexane at room temperature. The structures in the solid state are shown in Figure 10. The metal ions have been incorporated in the binding pocket of **4**. They are coordinated by the last free phosphine arm (P3), the central Sb atom, one carbonyl ligand [C1 (**19**, **20**) or C3 (**21**)] and for **19** and **20** saturated by one acetonitrile molecule. The bridging CO ligand of all three complexes gives rise to a band in the corresponding IR spectra shifted to lower wave numbers (**19**: 1805, **20**: 1832, **21**:1801 cm^{-1}).

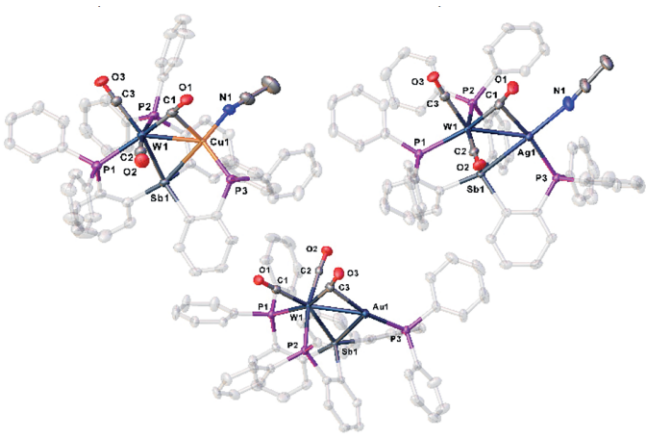

Figure 10. Structure in the solid state of **19** (top left), **20** (top right) and **21** (bottom). Anions, solvent molecules and hydrogen atoms are omitted for clarity.

The tungsten metal distances are 2.7922(7) (**19**), 2.8891(3) (**20**) and 2.7551(2) Å (**21**). The WBI values of 0.07 and 0.10, 0.17 for **19**, **20** and **21**, respectively, indicate the emergence of metal–metal bonding.

Conclusions

It could be shown that the ligands **L1**–**L3** can be easily introduced into tungsten and molybdenum carbonyl complexes. The tungsten complexes with incorporated ligand **L1** (*cis*-$[W(CO)_4\{(o\text{-}PPh_2C_6H_4)_3Sb\}]$ (**1**) and *fac*-$[W(CO)_3\{(o\text{-}PPh_2C_6H_4)_3Sb\}]$ (**4**)) provide binding pockets with several free phosphine arms, providing a site for the complexation of coinage metal ions. Copper, silver and gold salts containing coordinating (Cl^-) or weakly coordinating counterions ($[PF_6]^-$) were used. In all reactions, the metals ions are coordinated by one or two phosphine groups, respectively. They are also connected to the antimony atom and are thus located in proximity of the tungsten atom, leading to W···M (M = Cu, Ag, Au) distance below the sum of the corresponding van der Waals radii. The resulting products possessing Cl^- as a counterion tend to show longer W···M (M = Cu, Ag, Au) distances compared to those with $[PF_6]^-$ as a counterion. The compounds derived from **4** show in general shorter W···M contacts than those derived from **1**. The shortest W···M distances are observed in complexes of the general formula *fac*-$[W(CO)_2(\mu\text{-}CO)\{(o\text{-}PPh_2C_6H_4)_3Sb\}\{ML\}][PF_6]$ [M = Cu, L = MeCN (**19**), M = Ag, L = MeCN (**20**), M = Au (**21**)]. The strength of the interaction with the tungsten atom increases within the group (Cu < Ag < Au).

Experimental Section

Synthetic Procedures: All the manipulations were performed in an atmosphere of dry argon using standard glove-box and Schlenk techniques. All solvents were degassed and purified by standard procedures. The used silica had activation state 1. The compounds $[W(CO)_4(nbd)]$ (nbd = norbonadiene),[13] $[W(CO)_3(cht)]$ (cht = 1,3,5-cycloheptatriene),[14] $[Mo(CO)_3(cht)]$,[15] $(oPPh_2C_6H_4)_3Sb$ (**L1**),[4] $(o\text{-}PPh_2C_6H_4)_2SbPh$ (**L2**),[16] $(o\text{-}PPh_2C_6H_4)_2SbCl$ (**L3**)[17] and (tht)AuCl[18] (tht = tetrahydrothiophene) were prepared according to literature procedures. CuCl, $[Cu(MeCN)_4][PF_6]$, AgCl, $Ag[PF_6]$, $Tl[PF_6]$ were purchased commercially. The NMR spectra were recorded with a Bruker Avance 400 spectrometer (^1H: 400.13 MHz, ^{31}P: 161.976 MHz) with δ (in ppm) referenced to external $SiMe_4$ (^1H) and H_3PO_4 (^{31}P). IR spectra were measured with a Varian FTS-800 spectrometer with diamond ATR-unit. All mass spectra were recorded with a Finnigan MAT 95 mass spectrometer (LIFDI-MS) or with a ThermoQuest Finnigan MAT TSQ 7000 mass spectrometer (ESI-MS). The C, H analyses were measured with an Elementar Vario EL III apparatus.

Synthesis of *cis*-$[W(CO)_4\{(o\text{-}PPh_2C_6H_4)_3Sb\}]$ (1): $[W(CO)_4(nbd)]$ (128 mg, 0.33 mmol) and $(o\text{-}PPh_2C_6H_4)_3Sb$ (300 mg, 0.33 mmol) were weighed in together and dissolved in 100 mL thf. After heating the reaction mixture under reflux for 18 h it was cooled to room temperature and the solvent removed in vacuo. The obtained yellow solid was dissolved in thf and layered with pentane at room temperature. After a few days **1** could be obtained as clear yellow plates. The supernatant was decanted off, the resulting crystals were washed tree times with pentane und dried in vacuo. Yield 290 mg (72 %). **^1H NMR** ($[D_8]$thf, 25 °C): δ = 6.96–7.49 (several overlapping multiplets).**^{31}P NMR** ($[D_8]$thf, 25 °C): δ = –5.0 (s, 2P, PPh_2)), 56.9 (s, 1P, PPh_2-W). **$^{31}P\{^1H\}$ NMR** ($[D_8]$thf, 25 °C): δ = –5.0 (s, 2P, PPh_2), 56.9 (s, $^1J_{PW}$ = 229 Hz, 1P, PPh_2-W).**ATR-IR** (diamond crystal): $\tilde{\nu}$ = 2012 (vs, CO) 1898 (vs, CO), 1872 (s, CO) cm^{-1}. **LIFDI-MS** (dme): *m/z* = 1174.1 (100 %, $[M - CO]^+$), 675.0 (9 %, $(o\text{-}PPh_2C_6H_4)_2Sb^+$). **EA** $C_{58}H_{42}O_4P_3SbW$: calcd. C 57.98; H 3.52 %; found: C 58.23; H 3.57 %.

Synthesis of *cis*-$[W(CO)_4\{(o\text{-}PPh_2C_6H_4)_2SbPh\}]$ (2): $[W(CO)_4(nbd)]$ (268 mg, 0.69 mmol) and $(o\text{-}PPh_2C_6H_4)_2SbPh$ (500 mg, 0.69 mmol) were weighed in together and dissolved in 100 mL thf. After heating the reaction mixture under reflux for 18 h it was cooled to room temperature and the solvent removed in vacuo. The obtained yellow solid was dissolved in dichloromethane and layered with hexane at room temperature. After a few days **3** could be obtained as clear yellow plates. The supernatant was decanted off, the resulting crystals were

washed tree times with hexane und dried in vacuo. Yield 456 mg (65 %).**^{1}H NMR** (CD_2Cl_2, 25 °C): δ = 6.91 (m, 2 H), 7.11 (m, 4 H), 7.32 (m, 24 H), 7.52 (m, 2 H), 7.84 (m, 1 H).**^{31}P NMR** (CD_2Cl_2, 25 °C): δ = –4.7 (s, 1P, *P*Ph_2), 54.8 (s, $^1J_{PW}$ = 223 Hz, 1P, *P*Ph_2-W).**^{31}P{^{1}H} NMR** (CD_2Cl_2, 25 °C): δ = –4.7 (s, 1P, *P*Ph_2), 54.8 (s, $^1J_{PW}$ = 225, $^1J_{PC}$ = 42 Hz, 1P, *P*Ph_2-W). **ATR-IR** (diamond crystal): $\tilde{\nu}$ = 2008 (vs, CO) 1919 (m, CO), 1911 (m, CO), 1873 (s, CO) cm^{-1}. **LIFDI-MS** (dme): *m*/*z* = 990.0 (100 %, [M – CO]$^+$), 675.0 (2 %, (*o*-$PPh_2C_6H_4)_2Sb^+$), 508.0 (5 %, [M]$^{2+}$), 495.0 (1 %, [M – CO]$^{2+}$), 480.0 (1 %,[M-2CO]$^{2+}$). **EA** $C_{46}H_{33}O_4P_2SbW$: calcd: C 54.31; H 3.27 %; found: C 54.19; H 3.30 %.

Synthesis of *cis*-[W(CO)$_4${(*o*-$PPh_2C_6H_4)_2$SbCl}] (3): [W(CO)$_4$(nbd)] (57 mg, 0.15 mmol) and (*o*-$PPh_2C_6H_4)_2$SbCl (100 mg, 0.15 mmol) were weighed in together and dissolved in 100 mL thf. After heating the reaction mixture under reflux for 17 h it was cooled to room temperature and the solvent removed in vacuo. The obtained yellow solid was dissolved in CH_2Cl_2 and layered with hexane at room temperature. After a few days **4** could be obtained as clear yellow plates. The supernatant was decanted off, the resulting crystals were washed tree times with hexane und dried in vacuo. Yield: 99 mg (68 %).**^{1}H NMR** ([D_8]thf, 25 °C): δ = 6.77 (m, 2 H), 7.02–7.49 (several overlapping multiplets, 23 H), 7.53 (m, 3 H), 7.66 (m, 1 H), 7.83 (m, 1 H).**^{31}P NMR** ([D_8]thf, 25 °C): δ = –12.2 (s, 2P, *P*Ph_2)), 56.7 (s, $^1J_{PW}$ = 225 Hz,1P, *P*Ph_2-W). **^{31}P{^{1}H} NMR** ([D_8]thf, 25 °C): δ = –13.1 (s, 1P, *P*Ph_2), 55.7 (s, $^1J_{PW}$ = 225, $^1J_{PC}$ = 41 Hz, 1P, *P*Ph_2-W).**ATR-IR** (diamond crystal): $\tilde{\nu}$ = 2026 (vs, CO), 1939 (s,CO), 1916 (m, CO), 1889 (m, CO) cm^{-1}.**LIFDI-MS** (dme): *m*/*z* = 976.0 (100 %, [M]$^+$), 948.0 (60 %, [M – CO]$^+$). **EA** $C_{40}H_{28}O_4ClP_2SbW$: calcd. C 49.28; H 2.90 %; found: C 49.33; H 3.32 %.

Synthesis of *fac*-[W(CO)$_3${(*o*-$PPh_2C_6H_4)_3$Sb}] (4): (a) [W(CO)$_4$(nbd)] (128 mg, 0.33 mmol) and (*o*-$PPh_2C_6H_4)_3$Sb (300 mg, 0.33 mmol) were weighed in together and 100 mL decalin was added. The reaction mixture was stirred under reflux for 18 h, while the initial clear yellow solution turned to turbid brown. After cooling to room temperature the solvent was removed in vacuo. The brown residue was dissolved in thf and purified by column chromatography using silica (hexane, 15 × 2.5 cm). Using toluene a weak yellow fraction (compound **1**) followed by a brown intense fraction (compound **2**) could be obtained under high loss (column was strong colored afterwards). The solvent was removed in vacuo. The residue was dissolved in dichloromethane and layered with hexane at room temperature. After a few days **2** could be obtained as dark yellow blocks. The supernatant was decanted off and the resulting crystals were washed three times with hexane und dried in vacuo. Yield 42 mg (11 %).

(b) A solution of **1** (2.0 g, 1.66 mmol) in thf was radiated for 63 h using a mercury TQ 150 lamp, while the color of the initial clear yellow solution turned into brown. The ^{31}P NMR spectrum of the crude solution shows the formation of **2** in 83 % yield. The solvent was removed in in vacuo. The residue was dissolved in dichloromethane and silca was added. The solvent was removed in vacuo. The preabsorbed product was purified by column chromatography (silica, hexane, 13 × 4.5 cm). Using toluene, a brown fraction could be eluted under high loss (column strong colored after procedure). The solvent was removed in vacuo. The residue was dissolved in dichloromethane, an excess of hexane added and cooled to –80 °C to precipitate **2** as a dark yellow powder. The supernatant was decanted off, the resulting powder was washed tree times with hexane und dried in vacuo. Yield 530 mg (27 %).

(c) A solution of **1** (1.2 g, 1.32 mmol) and [W(CO)$_3$(cht)] (476 mg, 1.32 mmol) in thf was stirred under reflux for 24 h, while the color changed from red to dark yellow. The solvent was removed in vacuo, the residue dissolved in CH_2Cl_2 and layered with hexane. After a few days **2** could be obtained as dark yellow blocks. The supernatant was decanted off, the resulting crystals were washed three times with hexane und dried in vacuo. Yield: 826 mg (53 %). **^{1}H NMR** ([D_8]thf, 25 °C): δ = 6.85 (m, 8 H), 7.08 (m, 6 H), 7.19 (m, 14 H), 7.29 (m, 4 H), 7.40 (m, 4 H), 7.51 (m, 1 H), 7.57 (m, 2 H), 7.72 (m, 2 H), 7.95 (m, 1 H).**^{31}P NMR** ([D_8]thf, 25 °C): δ = –4.7 (s, 2P, *P*Ph_2), 57.8 (s, $^1J_{PW}$ = 220 Hz, 1P, *P*Ph_2-W).**^{31}P{^{1}H} NMR** ([D_8]thf, 25 °C): δ = –4.7 (s, 1P, *P*Ph_2), 57.8 (s, $^1J_{PW}$ = 216 Hz, 2P, *P*Ph_2-W). **ATR-IR** (diamond crystal): $\tilde{\nu}$ = 1935 (vs, CO) 1859 (s, CO), 1838 (s, CO) cm^{-1}. **LIFDI-MS** (dme): *m*/*z* = 1174.0 ([M]$^+$). **EA** $C_{57}H_{42}O_3P_3SbW$: calcd. C 58.34; H 3.61 %; found: C 58.33; H 3.77 %.

Synthesis of *fac*-[W(CO)$_3${(*o*-$PPh_2C_6H_4)_2$SbCl}] (5): [W(CO)$_4$(nbd)] (218 mg, 0.56 mmol) and (*o*-$PPh_2C_6H_4)_2$SbCl (383 mg, 0.56 mmol) were weighed in together and dissolved in 150 mL thf. After heating the reaction mixture under reflux for 18 h it was cooled to room temperature and radiated for 2 h with a mercury TQ 150 lamp. The initial yellow solution turned to orange. Silca was added and the solvent was removed in vacuo. The preabsorbed compound was purified by column chromatography using silica (hexane, 18 × 3.5 cm). Using toluene/hexane 1:3 a narrow weak yellow (**4**) and an orange fraction (**5**) could be eluted under high loss (column strong colored after procedure). The solvent was removed in vacuo, the residue dissolved in thf and layered with hexane. After a few days **5** could be obtained as orange plates. The supernatant was decanted off, the resulting crystals were washed tree times with hexane und dried in vacuo. Yield 37 mg (7 %).**^{1}H NMR** (CD_2Cl_2, 25 °C): δ = 6.81 (m, 4 H), 6.90 (m, 4 H), 7.14 (m, 3 H), 7.35 (m, 12 H), 7.66 (m, 3 H), 8.45 (m, 2 H). **^{31}P NMR** (CD_2Cl_2, 25 °C): δ = *52.4* (s, *P*Ph_2-W). **^{31}P{^{1}H} NMR** (CD_2Cl_2, 25 °C): δ = 52.4 (s, $^1J_{PW}$ = 212 Hz, *P*Ph_2-W). **ATR-IR** (diamond crystal): $\tilde{\nu}$ = 1948 (vs, CO), 1860 (s, CO) cm^{-1}. **LIFDI-MS** (dme): *m*/*z* = 948.0 (100 %, [M]$^+$). **EA** $C_{39}H_{28}O_3ClP_2SbW$: calcd. C 49.47; H 2.98 %; found: C 49.67; H 2.95 %.

Synthesis of *fac*-[(W(CO)$_3${(*o*-$PPh_2C_6H_4)_2$Sb})$_2$] (6): (a) [W(CO)$_4$(nbd)] (57 mg, 0.15 mmol) and (o-$PPh_2C_6H_4)_2$SbCl (100 mg, 0.15 mmol) were weighed in together and dissolved in 30 mL toluene. After heating the reaction mixture under reflux for 21 h it was cooled to room temperature. The initial yellow solution turned to brown. The solvent was removed in vacuo and the residue dissolved in CH_2Cl_2. After adding silica, the solvent was removed in vacuo. The preabsorbed compound was purified by column chromatography using silica (hexane, 15 × 2 cm). Using toluene a weak yellow (**4**) and a strong orange fraction (**6**) could be obtained under high loss (column strong colored afterwards). The solvent was removed in vacuo, the residue dissolved in thf and layered with pentane. After a few days **6** could be obtained as orange blocks. The supernatant was decanted off, the resulting crystals were washed tree times with pentane und dried in vacuo. Yield: only a few crystals could be isolated.

(b) [W(CO)$_4$(nbd)] (114 mg, 0.29 mmol) and (*o*-$PPh_2C_6H_4)_2$SbCl (200 mg, 0.29 mmol) were weighed in together and dissolved in 150 mL thf. After heating the reaction mixture under reflux for 18 h it was cooled to room temperature and radiated for 4 h with a mercury TQ 150 lamp. The initial yellow solution turned to orange. The ^{31}P NMR spectra of the reaction mixture shows the formation of **6** in 17 % and **5** in 54 % beside unidentified side products. Silca was added and the solvent was removed in vacuo. The preabsorbed compound was purified by column chromatography using silica (hexane, 18 × 3.5 cm). Using toluene/hexane 1:3 a narrow weak yellow (**5**) and an orange fraction (**5**) could be eluted under high loss (column strong colored after procedure). The solvent was removed in vacuo, the residue dis-

solved in thf and layered with hexane. After a few days **5** could be obtained as orange plates. The supernatant was decanted off, the resulting crystals were washed tree times with hexane und dried in vacuo. Yield: only a few crystals could be isolated. **^{1}H NMR** ([D$_8$]thf, 25 °C): δ = 6.87 (m, 8 H), 7.07–7.31 (several overlapping multiplets, 18 H), 8.38 (m, 2 H). **^{31}P NMR** ([D$_8$]thf, 25 °C): δ = 57.1 (s). **^{31}P{^{1}H} NMR** ([D$_8$]thf, 25 °C): δ = 57.1 (s, $^1J_{PW}$ = 104 Hz). **ATR-IR** (diamond crystal): $\tilde{\nu}$ = 1930 (vs, CO), 1844 (s, CO) cm^{-1}. **LIFDI-MS** (dme): *m*/*z* = 1823.9 (100 %, [M]$^+$), 675.0 (57 %, (*o*-PPh$_2$C$_6$H$_4$)$_2$Sb$^+$). **EA** C$_{78}$H$_{56}$O$_6$P$_4$Sb$_2$W$_2$: calcd. C 51.35; H 3.09 %; found: C 50.89; H 3.32 %.

Synthesis of *fac*-[Mo(CO)$_3${(*o*-PPh$_2$C$_6$H$_4$)$_3$Sb}] (7): [Mo(CO)$_3$(cht)] (60 mg, 0.22 mmol) and (o-PPh$_2$C$_6$H$_4$)$_3$Sb (200 mg, 0.22 mmol) were weighed in together and dissolved in 100 mL thf. After stirring the reaction mixture under reflux for 18 h the solvent was removed in vacuo. The yellow residue was dissolved in dichloromethane and layered with hexane at room temperature. After a few days **7** could be obtained as yellow blocks. The supernatant was decanted off, the resulting crystals were washed three times with hexane und dried in vacuo. Yield 137 mg (57 %). **^{1}H NMR** (CD$_2$Cl$_2$, 25 °C): δ = 6.83 (m, 4 H), 6.90 (m, 4 H), 7.09–7.42 (several overlapping multiplets, 28 H), 7.48–7.60 (several overlapping multiplets, 3 H), 7.66 (m, 2 H), 7.93 (m, 1 H). **^{31}P NMR** (CD$_2$Cl$_2$, 25 °C): δ = –6.3 (s, 1P, *P*Ph$_2$), 71.2 (s, 2P, *P*Ph$_2$-Mo). **^{31}P{^{1}H} NMR** (CD$_2$Cl$_2$, 25 °C): δ = –6.3 (s, 1P, *P*Ph$_2$), 71.2 (s, 2P, *P*Ph$_2$-Mo). **ATR-IR** (diamond crystal): $\tilde{\nu}$ = 1941 (vs, CO) 1866 (s, CO), 1845 (s, CO) cm^{-1}. **LIFDI-MS** (dme): *m*/*z* = 1086.0 (100 %, [M]$^+$), 1058.0.0 (6 %, [M – CO]$^+$). **EA** C$_{57}$H$_{42}$O$_3$P$_3$SbMo: calcd. C 63.06; H 3.90 %; found: C 62.92; H 4.10 %.

Synthesis of *fac*-[Mo(CO)$_3${(*o*-PPh$_2$C$_6$H$_4$)$_2$SbPh}] (8): [Mo(CO)$_3$(cht)] (75 mg, 0.28 mmol) and (*o*-PPh$_2$C$_6$H$_4$)$_2$SbPh (200 mg, 0.28 mmol) were weighed in together and dissolved in 100 mL thf. After stirring the reaction mixture under reflux for 16 h the solvent was removed in vacuo. The yellow residue was dissolved in dimethoxyethane and layered with hexane at room temperature. After a few days **8** could be obtained as yellow blocks. The supernatant was decanted off, the resulting crystals were washed three times with hexane und dried in vacuo. Yield 116 mg (47 %). **^{1}H NMR** ([D$_8$]thf, 25 °C): δ = 6.88 (m, 7 H), 7.08 (m, 3 H), 7.23–7.48 (several overlapping multiplets, 15 H), 7.56 (m, 3 H), 7.83 (m, 2 H), 7.99 (m, 3 H). **^{31}P NMR** ([D$_8$]thf, 25 °C): δ = 73.4 (s). **^{31}P{^{1}H} NMR** ([D$_8$]thf, 25 °C): δ = 73.4 (s). **ATR-IR** (diamond crystal): $\tilde{\nu}$ = 1928 (vs, CO), 1854 (s, CO), 1818 (s, CO) cm^{-1}. **LIFDI-MS** (dme): *m*/*z* = 902.0 (100 %, [M]$^+$). **EA** C$_{45}$H$_{33}$O$_3$P$_2$SbMo: calcd. C 59.96; H 3.69 %; found: C 59.82; H 3.79 %.

Synthesis of *fac*-[Mo(CO)$_3${(*o*-PPh$_2$C$_6$H$_4$)$_2$SbCl}] (9): [Mo(CO)$_3$(cht)] (264 mg, 0.97 mmol) and (o-PPh$_2$C$_6$H$_4$)$_2$SbCl (660 mg, 0.97 mmol) were weighed in together and dissolved in 200 mL thf. After stirring the reaction mixture under reflux for 18 h the solvent was removed in vacuo. The orange residue was dissolved in dichloromethane and layered with hexane at room temperature. After a few days **9** could be isolated as orange rods. The supernatant was decanted off and the resulting crystals were washed three times with hexane und dried in vacuo. Yield 208 mg (25 %). **^{1}H NMR** ([D$_8$]thf, 25 °C): δ = 6.83 (m, 4 H), 6.91 (m, 4 H), 7.15 (m, 2 H), 7.28–7.41 (several overlapping multiplets, 14 H), 7.67 (m, 2 H), 8.40 (m, 2 H). **^{31}P NMR** ([D$_8$]thf, 25 °C): δ = 66.6 (s). **^{31}P{^{1}H} NMR** ([D$_8$]thf, 25 °C): δ = 66.6 (s). **ATR-IR** (diamond crystal): $\tilde{\nu}$ = 1955 (vs, CO), 1885 (m, CO), 1866 (s, CO), m 1856 (s, CO) cm^{-1}.**LIFDI-MS** (dme): *m*/*z* = 859.8 (100 %, [M]$^+$). **EA** C$_{39}$H$_{28}$O$_3$P$_2$SbMo x 0.5 CH$_2$Cl$_2$: calcd. C 52.58; H 3.24 %; found: C 52.38; H 3.40 %.

Synthesis of *cis*-[W(CO)$_4${(*o*-PPh$_2$C$_6$H$_4$)$_3$Sb}{CuCl}] (10): CuCl (8.2 mg, 0.083 mmol, 1 equiv.) and **1** (100 mg, 0.083 mmol, 1 equiv.) were weighed in together and 20 mL CH$_2$Cl$_2$ was added. After stirring overnight, the solvent of the yellow solution was removed in vacuo. The residue was dissolved in CH$_2$Cl$_2$ and layered with hexane. After a few days, **10** can be obtained as dark yellow blocks. The supernatant was decanted off, the residue washed with hexane and dried in vacuo. Yield: 85 mg (79 %). **^{1}H NMR** (CD$_2$Cl$_2$, 25 °C): δ [ppm] = 7.81 (m, 1 H, *Ph*), 7.61–7.06 (m, 35 H, *Ph*), 7.04–6.88 (m, 6 H, *Ph*). **^{31}P{^{1}H} NMR** (CD$_2$Cl$_2$, 25 °C): δ [ppm] = 52.5 (s, 1P, $^1J_{PW}$ = 213 Hz, *P*W(CO)$_4$), –1.9 (s, 2P, *P*). **^{31}P NMR** (CD$_2$Cl$_2$, 25 °C): δ [ppm] = 52.5 (s, 1P, $^1J_{PW}$ = 213 Hz, *P*W(CO)$_4$), –1.9 (s, 2P, *P*). **LIFDI-MS** (dme): *m*/*z* = 1369.9 (4 %, [M + 2Cl]$^+$), 1237.0 (9 %, [M-Cu]$^+$), 1174.0 (100 %, [M-CuCl-CO]$^+$), 1146.0 (16 %, [M-CuCl-2CO]$^+$). **EA** C$_{58}$H$_{42}$O$_4$P$_3$SbWCuCl x 0.2 CH$_2$Cl$_2$: calcd. C 53.06; H 3.24; found C 53.19; H 3.38. **ATR-IR** (diamond crystal): $\tilde{\nu}$ = 2011 (vs, CO),1931 (m, CO), 1919 (m, CO), 1899 (m, CO), 1881 (w, CO), 1869 (w, CO) cm^{-1}.

Synthesis of *cis*-[W(CO)$_4${(*o*-PPh$_2$C$_6$H$_4$)$_3$Sb}{AgCl}] (11): AgCl (11.9 mg, 0.083 mmol, 1 equiv.) and **1** (100 mg, 0.083 mmol, 1 equiv.) were sonicated in CH$_2$Cl$_2$/MeCN (5:1) for 14 h. The ^{31}P{^{1}H} spectrum of the reaction mixture reveals a mixture of **11** and **1** (4:1). It was filtered through diatomaceous earth and the solvent removed in vacuo. The residue was dissolved in CH$_2$Cl$_2$ and layered with hexane. After a few days, **11** could be obtained as yellow flat rods beside yellow blocks of **1**. The solvent was decanted off, the crystals washed with hexane and dried in vacuo. According to NMR spectra and elemental analysis a 4:1 mixture of **11** and **2** is obtained. Yield: 49 mg (39.2 mg **11** (35 %), 9.9 mg **1**). **^{1}H NMR** (CD$_2$Cl$_2$, 25 °C): δ [ppm] = 7.92 (m, 1 H, *Ph*), 7.69 (m, 1 H, *Ph*), 7.58–6.78 (m, 40 H, *Ph*). **^{31}P{^{1}H} NMR** (CD$_2$Cl$_2$, 25 °C): δ [ppm] = 56.2 (s, 0.28P, $^1J_{PW}$ = 229 Hz, *P*W(CO)$_4$, **I**), 52.5 (s, 1P, $^1J_{PW}$ = 212 Hz, *P*W(CO)$_4$, **2**), 2.8 (d, 1P, ^{2}J$_{PP}$ = 17 Hz, *P*, **2**), 1.1 (d, 1P, ^{2}J$_{PP}$ = 17 Hz, *P*, **2**), –5.3 (s, 0.56P, *P*, **I**). **^{31}P NMR** (CD$_2$Cl$_2$, 25 °C): δ [ppm] = 56.2 (s, 0.24P, *P*W(CO)$_4$, **I**), 52.5 (s, 1P, $^1J_{PW}$ = 212 Hz, *P*W(CO)$_4$, **2**), 2.8 (s, 1P, *P*, **2**), 1.1 (s, 1P, *P*, **2**), –5.3 (s, 0.56P, *P*, **I**). **LIFDI-MS** (dme): *m*/*z* = 1309.1 (15 %, [M – Cl]$^+$), 1174.0 (100 %, [M-AgCl-CO]$^+$). **EA** (C$_{58}$H$_{42}$O$_4$P$_3$SbWAgCl)$_{0.8}$·(C$_{58}$H$_{42}$O$_4$P$_3$SbW)$_{0.2}$·1.3 CH$_2$Cl$_2$: calcd. C 50.66; H 3.16; found C 49.94; H 3.37. **ATR-IR** (diamond crystal): $\tilde{\nu}$ = 2025 (vs, CO), 1935 (s, CO), 1895 (vs, CO) cm^{-1}.

Synthesis of *cis*-[W(CO)$_4${(*o*-PPh$_2$C$_6$H$_4$)$_2$Sb}{AuCl(*o*-PPh$_2$C$_6$H$_4$)}{AuCl}] (12) and *cis*-[(W(CO)$_4${(*o*-PPh$_2$C$_6$H$_4$)$_2$Sb})$_2$AuCl] (13): A solution of (tht)AuCl (53.4 mg, 0.166 mmol, 2 equiv.) in 10 mL CH$_2$Cl$_2$ was added to a stirred solution of **1** (100 mg, 0.083 mmol, 1 equiv.) in 10 mL CH$_2$Cl$_2$ while the color changed to orange. The solvent was removed in vacuo after stirring for 30 minutes. The residue was dissolved in CH$_2$Cl$_2$ and layered with hexane. After a few days **12** can be obtained as orange plates beside very few dark blocks of **13**. The solvent was decanted off, washed with hexane and dried in vacuo. Compound **12**: Yield: 72 mg (52 %). **^{1}H NMR** (CD$_2$Cl$_2$, 25 °C): δ [ppm] = 8.04 (m, 2 H, *Ph*), 7.70–7.22 (m, 34 H, *Ph*), 7.15 (m, 2 H, *Ph*), 7.04 (m, 2 H, *Ph*), 6.83 (m, 2 H, *Ph*). **^{31}P{^{1}H} NMR** (CD$_2$Cl$_2$, 25 °C): δ [ppm] = 61.2 (d, 1P, $^2J_{PP}$ = 8 Hz, *P*), 54.2 (s, 1P, $^1J_{PW}$ = 221 Hz, *P*W(CO)$_4$), 34.6 (d, 1P, ^{2}J$_{PP}$ = 8 Hz, *P*). **^{31}P NMR** (CD$_2$Cl$_2$, 25 °C): δ [ppm] = 61.2 (s, 1P, *P*), 54.2 (s, 1P, $^1J_{PW}$ = 221 Hz, *P*W(CO)$_4$), 34.6 (s, 1P, *P*). **LIFDI-MS** (o-C$_6$H$_4$F$_2$): *m*/*z* = 1596.1 (20 %, [M – 2Cl]$^+$). **EA** C$_{58}$H$_{42}$O$_4$P$_3$SbWAu$_2$Cl$_2$: calcd. C 41.81; H 2.54 %; found C 42.08; H 2.87 %. **ATR-IR** (diamond crystal): $\tilde{\nu}$ = 2017 (vs, CO), 2005 (s, CO), 1922 (m, CO), 1904 (w, CO), 1868 (w, CO), 1845 (w, CO) cm^{-1}. Compound **13**: Yield: few crystals. **^{1}H NMR** (CD$_2$Cl$_2$, 25 °C): δ [ppm]

= 9.34 (m, 1 H, *Ph*) 8.59 (m, 1 H, *Ph*), 7.74 (m, 3 H, *Ph*), 7.64 (m, 5 H, *Ph*), 7.42–7.28 (m, 17 H, *Ph*), 7.18–6.75 (m, 14 H, *Ph*), 6.36 (m, 1 H, *Ph*). **^{31}P{^{1}H} NMR** (CD_2Cl_2, 25 °C): δ [ppm] = 54.8 (s, 1P, $^{1}J_{PW}$ = 218 Hz, *P*W(CO)$_4$), 40.4 (s, 1P, *P*). **^{31}P NMR** (CD_2Cl_2, 25 °C): δ [ppm] = 54.8 (s, 1P, $^{1}J_{PW}$ = 218 Hz, *P*W(CO)$_4$), 40.4 (s, 1P, *P*).

Synthesis of *cis*-[W(CO)$_4${(*o*-PPh$_2$C$_6$H$_4$)$_3$Sb}{Cu}][PF$_6$] (14): [Cu(MeCN)$_4$][PF$_6$] (31 mg, 0.083 mmol, 1 equiv.) and **1** (100 mg, 0.083 mmol, 1 equiv.) were weighed in together and 20 mL CH_2Cl_2 was added. After stirring overnight, the solvent of the yellow solution was removed in vacuo. The residue was dissolved in *o*-difluoro benzene and layered with hexane. After a few days, **14** can be obtained as dark yellow blocks. The supernatant was decanted off, the residue washed with hexane and dried in vacuo. Yield: 82 mg (70 %). **^{1}H NMR** (CD_2Cl_2, 25 °C): δ [ppm] = 8.51 (m, 1 H, *Ph*), 7.87 (m, 1 H, *Ph*), 7.71–6.99 (m, 36 H, *Ph*), 6.55 (m, 4 H, *Ph*). **^{31}P{^{1}H} NMR** (CD_2Cl_2, 25 °C): δ [ppm] = 49.4 (s, 1P, $^{1}J_{PW}$ = 199 Hz, *P*W(CO)$_4$), 5.8 (s, 2P, *P*), –143.9 (sept, 1P, $^{1}J_{PF}$ = 710 Hz, *P*F$_6$). **^{31}P NMR** (CD_2Cl_2, 25 °C): δ [ppm] = 49.4 (s, 1P, $^{1}J_{PW}$ = 199 Hz, *P*W(CO)$_4$), 5.8 (s, 2P, *P*), 143.9 (sept, 1P, $^{1}J_{PF}$ = 710 Hz, *P*F$_6$). **^{19}F NMR** (CD_2Cl_2, 25 °C): δ [ppm] = –73.4 (d, $^{1}J_{PF}$ = 710 Hz, P*F*$_6$). **ESI-MS** (CH_2Cl_2): *m*/*z* = 1265.0 (100 %, [M]$^+$). **EA** (C$_{58}$H$_{42}$O$_4$P$_4$SbWCuF$_6$·0.44 C$_6$H$_{14}$): calcd. C 50.30; H 3.35 %; found C 50.49; H 3.00 %. **ATR-IR** (diamond crystal): $\tilde{\nu}$ = 2032 (s, CO), 1943 (s, CO), 1928 (vs, CO), 1826 (m, CO) cm^{-1}.

Synthesis of *cis*-[W(CO)$_4${(*o*-PPh$_2$C$_6$H$_4$)$_3$Sb}{AgMeCN}][PF$_6$] (15): Ag[PF$_6$] (21 mg, 0.083 mmol, 1 equiv.) and **1** (100 mg, 0.083 mmol, 1 equiv.) were weighed in together, 20 mL CH_2Cl_2 and 1 mL MeCN were added. After stirring overnight, the solvent of the yellow solution was removed in vacuo. The residue was dissolved in CH_2Cl_2 and layered with hexane. After a few days, **15** can be obtained as bright yellow blocks. The supernatant was decanted off, the residue washed with hexane and dried in vacuo. Yield: 86 mg (69 %). **^{1}H NMR** (CD_2Cl_2, 25 °C): δ [ppm] = 8.20 (m, 1 H, *Ph*), 7.75 (m, 1 H, *Ph*), 7.64 (m, 2 H, *Ph*), 7.52–7.10 (m, 32 H, *Ph*), 7.00 (m, 2 H, *Ph*), 6.86 (m, 2 H, *Ph*), 1.98 (s, 3 H, C*H*$_3$CN). **^{31}P{^{1}H} NMR** (CD_2Cl_2, 25 °C): δ [ppm] = 50.6 (s, 1P, $^{1}J_{PW}$ = 202 Hz, *P*W(CO)$_4$), 9.8 (d, 1P, $^{2}J_{PP}$ = 25 Hz, *P*), 7.6 (d, 1P, $^{2}J_{PP}$ = 25 Hz, *P*), –143.9 (sept, 1P, $^{1}J_{PF}$ = 710 Hz, *P*F$_6$). **^{31}P NMR** (CD_2Cl_2, 25 °C): δ [ppm] = 50.6 (s, 1P, $^{1}J_{PW}$ = 202 Hz, *P*W(CO)$_4$), 9.8 (d, 1P, $^{2}J_{PP}$ = 25 Hz, *P*), 7.6 (d, 1P, $^{2}J_{PP}$ = 25 Hz, *P*), –143.9 (sept, 1P, $^{1}J_{PF}$ = 710 Hz, *P*F$_6$). **^{19}F NMR** (CD_2Cl_2, 25 °C): δ [ppm] = –73.4 (d, $^{1}J_{PF}$ = 710 Hz, P*F*$_6$). **ESI-MS** (CH_2Cl_2): *m*/*z* = 1309.0 (100 %, [M-MeCN]$^+$). **EA** (C$_{60}$H$_{45}$O$_4$NP$_4$SbWAgF$_6$): calcd. C 48.19; H 3.03; N 0.94 %; found C 48.09; H 3.05; N 0.83 %. **ATR-IR** (diamond crystal): $\tilde{\nu}$ = 2021 (s, CO), 1924 (m, CO), 1902 (vs, CO) cm^{-1}.

Synthesis of *cis*-[W(CO)$_4${(*o*-PPh$_2$C$_6$H$_4$)$_3$Sb}{Au}][PF$_6$] (16): A solution of (tht)AuCl (26.7 mg, 0.083 mmol, 1 equiv.) was added to a stirred solution of **1** (100 mg, 0.083 mmol, 1 equiv.) and TlPF$_6$ (29.1 mg, 0.083 mmol, 1 equiv.) in CH_2Cl_2. After a few minutes the color changed to orange and a bright precipitate (TlCl) was obtained. After stirring for one hour, it was filtered through diatomaceous earth. The solvent was removed in vacuo, the residue dissolved in CH_2Cl_2 and layered with hexane. After a few days, **16** can be obtained as dark yellow blocks. The supernatant was decanted off, the crystals washed with hexane and dried in vacuo. Yield: 88 mg (69 %). **^{1}H NMR** (CD_2Cl_2, 25 °C): δ [ppm] = 8.45 (m, 1 H, *Ph*), 7.80 (m, 5 H, *Ph*), 7.62 (m, 11 H, *Ph*), 7.45 (m, 3 H, *Ph*), 7.32 (m, 10 H, *Ph*), 7,15 (m, 8 H, *Ph*), 6.64 (m, 4 H, *Ph*). **^{31}P{^{1}H} NMR** (CD_2Cl_2, 25 °C): δ [ppm] = 52.1 (s, 1P, $^{1}J_{PW}$ = 197 Hz, *P*W(CO)$_4$), 43.8 (s, 2P, *P*), –143.9 (sept, 1P, $^{1}J_{PF}$ = 710 Hz, *P*F$_6$). **^{31}P NMR** (CD_2Cl_2, 25 °C): δ [ppm] = 52.1 (s, 1P, $^{1}J_{PW}$ = 197 Hz, *P*W(CO)$_4$), 43.8 (s, 2P, *P*), –143.9 (sept, 1P, $^{1}J_{PF}$ = 710 Hz, *P*F$_6$). **^{19}F NMR** (CD_2Cl_2, 25 °C): δ [ppm] = –73.4 (d, $^{1}J_{PF}$ = 710 Hz, P*F*$_6$). **ESI-MS** (CH_2Cl_2): *m*/*z* = 1399.1 (100 %, [M]$^+$). **EA** (C$_{58}$H$_{42}$O$_4$P$_4$SbWAuF$_6$·0.9 CH_2Cl_2): calcd. C 43.67; H 2.73 %; found C 43.70; H 2.89 %. **ATR-IR** (diamond crystal): $\tilde{\nu}$ = 2025 (s, CO), 1914 (m, CO), 1882 (vs, CO) cm^{-1}.

Synthesis of *cis*-[W(CO)$_2$(μ-CO){(*o*-PPh$_2$C$_6$H$_4$)$_3$Sb}{Cu$_2$(μ-Cl)$_2$}] (17): CuCl (16.8 mg, 0.170 mmol, 2 equiv.) and **4** (100 mg, 0.085 mmol, 1 equiv.) were weighed in together, 20 mL CH_2Cl_2 and 1 mL MeCN were added. After stirring overnight, the solvent of the yellow solution was removed in vacuo. The residue was dissolved in CH_2Cl_2 and layered with hexane. After a few days, **17** can be obtained as orange plates. The supernatant was decanted off, the residue washed with hexane and dried in vacuo. Yield: 102 mg (88 %). **^{1}H NMR** (CD_2Cl_2, 25 °C): δ [ppm] = 7.61 (m, 2 H, *Ph*), 7.53–7.21 (m, 23 H, *Ph*), 7.14 (m, 7 H, *Ph*), 7.02 (m, 2 H, *Ph*), 6.96 (m, 1 H, *Ph*), 6.88 (m, 5 H, *Ph*), 6.67 (m, 1 H, *Ph*). **^{31}P{^{1}H} NMR** (CD_2Cl_2, 25 °C): δ [ppm] = 59.9 (s, 1P, $^{1}J_{PW}$ = 212 Hz, *P*W(CO)$_4$), 14.0 (s, 1P, *P*), 5.5 (s, 1P, *P*). **^{31}P NMR** (CD_2Cl_2, 25 °C): δ [ppm] = 59.9 (s, 1P, $^{1}J_{PW}$ = 212 Hz, *P*W(CO)$_4$), 14.0 (s, 1P, *P*), 5.5 (s, 1P, *P*). **LIFDI-MS** (o-C$_6$H$_4$F$_2$): *m*/*z* = 1372.0 (21 %, [M]$^+$), 1237.1 (20 %, [M-Cu-2Cl]$^+$), 1174.2 (100 %, [M-2Cu-2Cl]$^+$), 1149.2 (21 %, [M-2Cu-2Cl-CO]$^+$). **EA** (C$_{57}$H$_{42}$O$_3$P$_3$SbWCu$_2$Cl$_2$): calcd. C 49.92; H 3.09 %; found C 49.98; H 3.18 %. **ATR-IR** (diamond crystal): $\tilde{\nu}$ = 1934 (vs, CO), 1846 (m, CO), 1801 (w, CO) cm^{-1}.

Synthesis of *fac*-[W(CO)$_3${(*o*-PPh$_2$C$_6$H$_4$)$_3$Sb}{AuCl}] (18): (tht) AuCl (27.3 mg, 0.085 mmol, 1 equiv.) in CH_2Cl_2 was added to a stirred solution of **4** (100 mg, 0.085 mmol, 1 equiv.) in CH_2Cl_2. After stirring for 5 hours, the solvent of the yellow solution was removed in vacuo. The residue was dissolved in CH_2Cl_2 and layered with hexane. After a few days, **18** can be obtained as bright yellow needles. The supernatant was decanted off, the residue washed with hexane and dried in vacuo. Yield: 37 mg (40 %). **^{1}H NMR** (CD_2Cl_2, 25 °C): δ [ppm] = 8.20 (m, 1 H, *Ph*), 7.82–6.50 (m, 41 H, *Ph*). **^{31}P{^{1}H} NMR** (CD_2Cl_2, 25 °C): δ [ppm] = 59.3 (br., $\omega_{1/2}$ = 142 Hz, 1P, *P*W(CO)$_4$), 50.2 (br., $\omega_{1/2}$ = 202 Hz,1P, *P*W(CO)$_4$), 30.6 (s, 1P, *P*). **^{31}P NMR** (CD_2Cl_2, 25 °C): δ [ppm] = 59.2 (br., $\omega_{1/2}$ = 220 Hz, 1P, *P*W(CO)$_4$), 50.2 (br., $\omega_{1/2}$ = 213 Hz,1P, *P*W(CO)$_4$), 30.6 (s, 1P, *P*). **LIFDI-MS** (o-C$_6$H$_4$F$_2$): *m*/*z* = 1371.2 (26 %, [M – Cl]$^+$), 1174.2 (100 %, [M-Au-Cl]$^+$). **EA** (C$_{57}$H$_{42}$O$_3$P$_3$SbWAuCl): calcd. C 48.70; H 3.01 %; found C 48.63; H 3.01 %. **ATR-IR** (diamond crystal): $\tilde{\nu}$ = 1931 (vs, CO), 1859 (s, CO), 1828 (m, CO) cm^{-1}.

Synthesis of *fac*-[W(CO)$_2$(μ-CO){(*o*-PPh$_2$C$_6$H$_4$)$_3$Sb}{CuMeCN}][PF$_6$] (19): [Cu(MeCN)$_4$][PF$_6$] (31.7 mg, 0.085 mmol, 1 equiv.) and **4** (100 mg, 0.085 mmol, 1 equiv.) were weighed in together and 20 mL CH_2Cl_2 was added. After stirring for 1 hour, the solvent of the yellow solution was removed in vacuo. The residue was dissolved in CH_2Cl_2 and layered with hexane. After a few days, **19** can be obtained as yellow blocks. The supernatant was decanted off, the residue washed with hexane and dried in vacuo. Yield: 80 mg (66 %). **^{1}H NMR** (CD_2Cl_2, 25 °C): δ [ppm] = 8.24 (m, 1 H, *Ph*), 7.83 (m, 2 H, *Ph*), 7.61 (m, 1 H, *Ph*), 7.39 (m, 18 H, *Ph*), 7.20 (m, 12 H, *Ph*), 6.93 (m, 4 H, *Ph*), 6.61 (m, 4 H, *Ph*), 1.98 (s, 3 H, C*H*$_3$CN). **^{31}P{^{1}H} NMR** (CD_2Cl_2, 25 °C): δ [ppm] = 59.9 (s, 2P, $^{1}J_{PW}$ = 212 Hz, *P*W(CO)$_4$), –4.1 (s, 1P, *P*), –143.9 (sept, 1P, $^{1}J_{PF}$ = 710 Hz, *P*F$_6$). **^{31}P NMR** (CD_2Cl_2, 25 °C): δ [ppm] = 59.9 (s, 2P, $^{1}J_{PW}$ = 212 Hz, *P*W(CO)$_4$), –4.1 (s, 1P, *P*), –143.9 (sept, 1P, $^{1}J_{PF}$ = 710 Hz, *P*F$_6$). **^{19}F NMR** (CD_2Cl_2, 25 °C): δ [ppm] = –73.4 (d, $^{1}J_{PF}$ = 710 Hz, P*F*$_6$). **ESI-MS** (CH_2Cl_2): *m*/*z* = 1273.0 (100 %, [M-MeCN]$^+$). **ATR-IR** (diamond crystal): $\tilde{\nu}$ = 1945 (s, CO), 1870 (s, CO), 1840 (vs, CO), 1805 (w, CO) cm^{-1}.

Synthesis of *fac*-[W(CO)$_2$(μ-CO){(*o*-PPh$_2$C$_6$H$_4$)$_3$Sb}{AgMeCN}][PF$_6$] (20): Ag[PF$_6$] (21.5 mg, 0.085 mmol, 1 equiv.) and **4** (100 mg, 0.085 mmol, 1 equiv.) were weighed in together, 20 mL CH_2Cl_2 and 1 mL MeCN were added. After stirring for 3 hours, the solvent of the yellow solution was removed in vacuo. The residue was dissolved in CH_2Cl_2 and layered with hexane. After a few days, **20** can be obtained as yellow needles. The supernatant was decanted off, the residue washed with hexane and dried in vacuo. Yield: 86 mg (70 %). **^{1}H NMR** (CD_2Cl_2, 25 °C): δ [ppm] = 7.83 (m, 2 H, *Ph*), 7.59 (m, 1 H, *Ph*), 7.54–7.11 (m, 30 H, *Ph*), 6.98 (m, 4 H, *Ph*), 6.62 (m, 4 H, *Ph*), 1.96 (s, 3 H, C*H*$_3$CN). **^{31}P{^{1}H} NMR** (CD_2Cl_2, 25 °C): δ [ppm] = 53.8 (br., 2P,, *P*W(CO)$_4$), 1.4 (dd, $^2J_{PP}$ = 33, $^2J_{PP}$ = 468 Hz, 1P, *P*), –143.9 (sept, 1P, $^1J_{PF}$ = 710 Hz, *P*F$_6$). **^{31}P NMR** (CD_2Cl_2, 25 °C): δ [ppm] = 53.8 (br., 2P,, *P*W(CO)$_4$), 1.4 (d, $^2J_{PP}$ = 468 Hz, 1P, *P*), –143.9 (sept, 1P, $^1J_{PF}$ = 710 Hz, *P*F$_6$). **^{19}F NMR** (CD_2Cl_2, 25 °C): δ [ppm] = –73.4 (d, $^1J_{PF}$ = 710 Hz, P*F*$_6$). **ESI-MS** (CH_2Cl_2): *m*/*z* = 1281.0 (100 %, [M-MeCN]$^+$). **EA** ($C_{59}H_{45}NO_3F_6P_4SbWAg$ x 0.5 CH_2Cl_2): calcd. C 47.89; H 3.11; N 0.94 %; found C 47.79; H 3.09; N 0.93 %. **ATR-IR** (diamond crystal): $\tilde{\nu}$ = 1954 (vs, CO), 1890 (s, CO), 1886 (s, CO), 1846 (s, CO), 1839 (s, CO), 1832 (s, CO) cm^{-1}.

Synthesis of *fac*-[W(CO)$_2$(μ-CO){(*o*-PPh$_2$C$_6$H$_4$)$_3$Sb} {Au}][PF$_6$] (21): Tl[PF$_6$] (29.8 mg, 0.085 mmol, 1 equiv.) and **4** (100 mg, 0.085 mmol, 1 equiv.) were weighed in together and 20 mL CH_2Cl_2 was added. A solution of (tht)AuCl (27.3 mg, 0.085 mmol, 1 equiv.) in 10 mL CH_2Cl_2 was added. After stirring for 2 hours, the turbid (TlCl) yellow solution was filtered through diatomaceous earth and the solvent removed in vacuo. The residue was dissolved in CH_2Cl_2 and layered with hexane. After a few days, **21** can be obtained as yellow plates. The supernatant was decanted off, the residue washed with hexane and dried in vacuo. Yield: 85 mg (66 %). **^{1}H NMR** (CD_2Cl_2, 25 °C): δ [ppm] = 8.35 (m, 1 H, *Ph*), 7.91 (m, 2 H, *Ph*), 7.62 (m, 2 H, *Ph*), 7.48 (m, 13 H, *Ph*), 7.30 (m, 16 H, *Ph*), 6.99 (m, 4 H, *Ph*), 6.67 (m, 4 H, *Ph*). **^{31}P{^{1}H} NMR** (CD_2Cl_2, 25 °C): δ [ppm] = 51.5 (s, 2P, $^1J_{PW}$ = 192 Hz, *P*W(CO)$_4$), 35.9 (s, 1P, *P*), –143.9 (sept, 1P, $^1J_{PF}$ = 710 Hz, *P*F$_6$). **^{31}P NMR** (CD_2Cl_2, 25 °C): δ [ppm] = 51.5 (s, 2P, $^1J_{PW}$ = 192 Hz, *P*W(CO)$_4$), 35.9 (s, 1P, *P*), –143.9 (sept, 1P, $^1J_{PF}$ = 710 Hz, *P*F$_6$). **^{19}F NMR** (CD_2Cl_2, 25 °C): δ [ppm] = –73.4 (d, $^1J_{PF}$ = 710 Hz, P*F*$_6$). **ESI-MS** (CH_2Cl_2): *m*/*z* = 1371.1 (100 %, [M]$^+$). **EA** ($C_{57}H_{42}O_3F_6P_4SbWAu$): calcd. C 45.18; H 2.79 %; found C 45.35; H 2.88 %. **ATR-IR** (diamond crystal): $\tilde{\nu}$ = 1966 (vs, CO), 1905 (s, CO), 1809 (s, CO), 1801 (s, CO) cm^{-1}.

Crystal Structure Determination: The X-ray diffraction experiments were performed on either an Gemini Ultra diffractometer (Oxford diffraction) with an AtlasS2 detector with Mo radiation (λ = 0.71073 Å)

Table 1. Crystallographic data and structure refinement data for **1**–**6**.

	1	**2**	**3**	**4**	**5**	**6**
Formula	$C_{116}H_{84}O_8P_6Sb_2W_2$	$C_{46}H_{33}O_4P_2SbW$	$C_{43}H_{35}ClO_4P_2SbW$	$C_{57}H_{42}O_3P_3SbW$	$C_{39.8}H_{29.6}Cl_{2.6}O_3P_2SbW$	$C_{41.25}H_{32}Cl_{2.5}N_{0.5}O_3P_2SbW$
$D_{calcd.}$ /g·cm^{-3}	1.623	1.716	1.782	1.631	1.797	1.755
μ /mm^{-1}	9.914	3.730	12.950	10.172	14.094	3.901
Formula weight	2402.85	1017.26	1018.70	1173.41	1015.54	1038.84
Color	clear light yellow	clear light yellow	clear light yellow	clear dark yellow	clear dark yellow	clear light orange
Shape	block	plate	trapezoid	block	block	block
Size /mm^3	0.25 × 0.23 × 0.19	0.27 × 0.22 × 0.12	0.25 × 0.15 × 0.09	0.19 × 0.12 × 0.07	0.32 × 0.20 × 0.05	0.33 × 0.22 × 0.14
T /K	122.98(10)	123.00(10)	123	122.96(15)	122.99(17)	123
Crystal system	monoclinic	monoclinic	triclinic	monoclinic	monoclinic	monoclinic
Space group	$P2_1/c$	$P2_1/n$	$P\bar{1}$	$P2_1/n$	$P2_1/n$	$P2_1/c$
a /Å	18.3796(2)	18.8878(3)	10.3754(3)	12.8041(3)	10.6955(2)	14.4324(3)
b /Å	13.7807(2)	16.48880(10)	11.2282(4)	19.1831(4)	25.2806(3)	18.4715(4)
c /Å	39.0326(4)	26.4002(3)	17.2897(5)	19.5342(3)	13.8876(2)	15.6431(4)
α /°	90	90	83.577(2)	90	90	90
β /°	95.7430(10)	106.6930(10)	81.021(3)	95.213(2)	90.906(2)	109.512(3)
γ /°	90	90	73.019(3)	90	90	90
V /Å^3	9836.7(2)	7875.50(17)	1898.09(11)	4778.19(17)	3754.58(10)	3930.77(17)
Z	4	8	2	4	4	4
Z′	1	2	1	1	1	1
Wavelength /Å	1.54184	0.71073	1.54184	1.54184	1.54184	0.71073
Radiation type	Cu-K_α	Mo-K_α	Cu-K_α	Cu-K_α	Cu-K_α	Mo-K_α
θ_{min} /°	2.416	3.319	4.127	3.236	3.497	3.328
θ_{max} /°	74.243	32.100	66.314	74.130	74.930	30.034
Measured refl.	54761	58372	23610	26389	40593	34305
Independent refl.	19320	24951	6652	9301	7542	11473
Reflections with $I > 2(I)$	17424	20253	6310	8216	7407	9667
R_{int}	0.0634	0.0353	0.0384	0.0823	0.0601	0.0292
Parameters	1207	973	442	586	424	501
Restraints	0	0	0	0	0	26
Largest peak	3.133	1.735	1.944	2.230	1.281	1.298
Deepest hole	–1.953	–1.372	–0.695	–3.806	–1.196	–1.225
GooF	1.054	1.040	1.049	1.028	1.050	1.072
wR_2 (all data)	0.1419	0.0721	0.0547	0.1311	0.0845	0.0731
wR_2	0.1372	0.0654	0.0538	0.1254	0.0841	0.0692
R_1 (all data)	0.0569	0.0479	0.0250	0.0565	0.0314	0.0410
R_1	0.0527	0.0327	0.0232	0.0507	0.0310	0.0301

Table 2. Crystallographic data and structure refinement data for **7**–**12**.

	7	**8**	**9**	**10**	**11**	**12**
Formula	$C_{57}H_{42}MoO_3P_3Sb$	$C_{45}H_{33}MoO_3P_2Sb$	$C_{39.8}H_{29.6}Cl_{2.6}MoO_3P_2Sb$	$C_{60}H_{46}Cl_5CuO_4P_3SbW$	$Ag_2C_{119}Cl_8H_{90}O_8P_6Sb_2W_2$	$C_{64}H_{46}Au_2Cl_2F_2O_4P_3SbW$
D_{calcd} /g·cm^{-3}	1.506	1.613	1.647	1.740	1.774	2.043
μ /mm^{-1}	7.920	9.682	1.366	3.269	13.437	7.727
Formula weight	1085.50	901.34	927.63	1470.27	2944.26	1780.35
Color	clear light yellow	clear dark yellow	clear light orange	clear dark yellow	clear light yellow	clear orange
Shape	block	block	block	block	needle	needle
Size /mm^3	0.43 × 0.28 × 0.22	0.38 × 0.28 × 0.20	0.53 × 0.33 × 0.24	0.65 × 0.40 × 0.29	0.50 × 0.12 × 0.05	0.38 × 0.07 × 0.05
T /K	123.01(10)	123.00(10)	123	123	123	123
Crystal system	monoclinic	monoclinic	monoclinic	monoclinic	monoclinic	triclinic
Space group	$P2_1/n$	$P2_1/n$	$P2_1/n$	$P2_1/n$	$P2_1/n$	$P\bar{1}$
a /Å	12.8125(2)	14.7738(2)	10.6890(2)	13.35920(10)	10.59820(10)	13.6227(2)
b /Å	19.1860(2)	14.9907(2)	25.2311(5)	22.84920(10)	23.01660(10)	14.1314(2)
c /Å	19.5578(2)	16.8603(2)	13.8729(2)	18.60380(10)	45.4915(3)	15.5884(3)
α /°	90	90	90	90	90	98.8900(10)
β /°	95.1950(10)	96.3120(10)	90.615(2)	98.7670(10)	96.4710(10)	95.1060(10)
γ /°	90	90	90	90	90	100.5170(10)
V /Å^3	4787.96(10)	3711.41(8)	3741.24(12)	5612.41(6)	11026.25(14)	2893.73(8)
Z	4	4	4	4	4	2
Z′	1	1	1	1	1	1
Wavelength /Å	1.54184	1.54184	0.71073	0.71073	1.54184	0.71073
Radiation type	Cu-K_α	Cu-K_α	Mo-K_α	Mo-K_α	Cu-K_α	Mo-K_α
θ_{min} /°	3.966	3.778	3.352	3.359	3.841	3.191
θ_{max} /°	67.079	67.065	30.033	37.725	66.796	28.282
Measured refl.	25339	38147	55003	166559	114070	26189
Independent refl.	8502	6625	10930	28895	19436	14330
Reflections with $I > 2(I)$	8269	6602	9957	25790	17750	12534
R_{int}	0.0441	0.0492	0.0245	0.0297	0.0477	0.0219
Parameters	586	469	478	676	1297	721
Restraints	0	0	69	0	0	3
Largest peak	2.790	1.752	1.051	2.529	1.177	1.399
Deepest hole	–1.586	–1.158	–0.775	–1.117	–0.924	–0.981
GooF	1.087	1.075	1.078	1.077	1.016	1.025
wR_2 (all data)	0.1196	0.1046	0.0573	0.0537	0.0699	0.0561
wR_2	0.1187	0.1046	0.0558	0.0519	0.0677	0.0534
R_1 (all data)	0.0447	0.0394	0.0278	0.0297	0.0314	0.0354
R_1	0.0439	0.0394	0.0237	0.0237	0.0278	0.0276

Table 3. Crystallographic data and structure refinement data for **13**–**18**.

	13	**14**	**15**	**16**	**17**	**18**
Formula	$AuC_{88.4}ClH_{75.6}O_8P_4Sb_2W_2$	$C_{68.5}CuF_6H_{66.5}O_4P_4SbW$	$C_{61.35}H_{47.7}AgCl_{2.7}F_6NO_4P_4SbW$	$Au_2C_{132}Cl_8F_{12}H_{120}O_8P_8Sb_2W_2$	$C_{59.77}H_{47.54}Cl_{7.54}Cu_2O_3P_3SbW$	$C_{57}H_{42}AuClO_3P_3SbW$
D_{calcd} /g·cm^{-3}	1.860	1.717	1.773	1.936	1.796	1.878
μ /mm^{-1}	15.379	6.711	12.221	10.762	12.099	15.661
Formula weight	2233.38	1560.73	1609.97	3598.77	1606.748	1405.83
Color	clear dark red	clear light yellow	clear light yellow	clear dark yellow	clear light red	clear light yellow
Shape	needle	block	block	block	block	plate
Size /mm^3	0.38 × 0.09 × 0.07	0.42 × 0.16 × 0.10	0.59 × 0.27 × 0.11	0.45 × 0.29 × 0.24	0.27 × 0.17 × 0.12	0.26 × 0.11 × 0.04
T /K	123	123.00(10)	123(1)	123.00(10)	123(1)	123(1)
Crystal system	monoclinic	monoclinic	triclinic	triclinic	monoclinic	monoclinic
Space group	$I2/a$	$P2_1/n$	$P\bar{1}$	$P\bar{1}$	$P2_1/n$	$P2_1$
a /Å	28.1784(3)	13.3553(2)	10.5734(4)	11.00250(10)	15.3444(3)	10.41326(5)
b /Å	13.84420(10)	23.2911(3)	13.0750(4)	23.9970(3)	18.8371(4)	21.09731(12)
c /Å	22.3139(2)	19.5328(2)	22.9061(9)	25.0343(3)	20.9101(4)	11.32988(5)
α /°	90	90	77.347(3)	105.5160(10)	90	90
β /°	113.6000(10)	96.5640(10)	88.149(3)	97.3420(10)	100.521(2)	93.0015(4)
γ /°	90	90	77.493(3)	99.6290(10)	90	90
V /Å^3	7976.77(14)	6036.04(13)	3016.10(19)	6174.68(13)	5942.3(2)	2485.67(2)
Z	4	4	2	2	4	2
Z′	0.5	1	1	1	1	1
Wavelength /Å	1.54184	1.39222	1.54184	1.39222	1.54184	1.54184
Radiation type	Cu-K_α	Cu-K_β	Cu-K_α	Cu-K_β	Cu-K_α	Cu-K_α
θ_{min} /°	3.423	2.676	3.547	2.775	3.75	3.907
θ_{max} /°	67.079	74.495	72.967	74.047	72.77	74.602
Measured refl.	32543	49535	21886	132102	32964	65955
Independent refl.	7130	16358	11634	33606	11556	9760
Reflections with $I > 2(I)$	6999	15894	10723	32877	10726	9647
R_{int}	0.0314	0.0282	0.0392	0.0400	0.0458	0.0593
Parameters	443	786	800	1621	757	604
Restraints	0	384	75	313	42	1
Largest peak	0.647	1.396	2.925	1.115	4.0909	1.268
Deepest hole	–0.907	–2.112	–1.883	–1.140	–3.2619	–0.641
GooF	1.083	1.196	1.069	1.150	1.0518	1.028
wR_2 (all data)	0.0466	0.1219	0.1066	0.0675	0.1279	0.0524
wR_2	0.0463	0.1215	0.1038	0.0671	0.1254	0.0522
R_1 (all data)	0.0196	0.0549	0.0434	0.0292	0.0603	0.0221
R_1	0.0191	0.0540	0.0400	0.0284	0.0561	0.0217
Flack parameter						–0.015(3)
Hooft parameter						–0.030(3)

Table 4. Crystallographic data and structure refinement data for **19**–**21**.

	19	**20**	**21**
Formula	$C_{59}H_{45}CuF_6NO_3P_4SbW$	$C_{60.65}H_{47.82}AgCl_{1.38}F_6N_{1.48}O_3P_4SbW$	$C_{58.7}H_{45.4}AuCl_{3.4}F_6O_3P_4SbW$
D_{calcd} /g•cm^{-3}	1.757	1.746	1.872
μ /mm^{-1}	7.476	11.957	5.215
Formula weight	1422.98	1545.61	1659.72
Color	clear light yellow	clear light yellow	clear light yellow
Shape	block	needle	block
Size /mm^3	$0.16 \times 0.09 \times 0.07$	$0.41 \times 0.08 \times 0.05$	$0.68 \times 0.33 \times 0.29$
T /K	123.01(11)	123	123
Crystal system	triclinic	monoclinic	monoclinic
Space group	$P\bar{1}$	$P2_1/n$	$P2_1/n$
a /Å	9.2830(3)	14.7149(3)	14.7854(3)
b /Å	13.3463(5)	19.7407(4)	19.7226(3)
c /Å	22.0387(9)	20.7094(4)	20.6640(5)
α /°	88.054(3)	90	90
β /°	81.984(3)	102.179(2)	102.232(2)
γ /°	84.411(3)	90	90
V /Å^3	2690.35(17)	5880.3(2)	5889.0(2)
Z	2	4	4
Z′	1	1	1
Wavelength /Å	1.39222	1.54184	0.71073
Radiation type	Cu-K_β	Cu-K_α	Mo-K_α
θ_{min} /°	3.005	3.802	3.353
θ_{max} /°	74.796	72.877	32.246
Measured refl.	30452	23452	35548
Independent refl.	14594	11378	18696
Reflections with $I > 2(I)$	12918	10474	15484
R_{int}	0.0367	0.0289	0.0236
Parameters	689	913	793
Restraints	0	550	144
Largest peak	1.991	1.474	2.821
Deepest hole	–1.613	–0.673	–1.127
GooF	1.031	1.058	1.087
wR_2 (all data)	0.1185	0.0722	0.0821
wR_2	0.1129	0.0702	0.0766
R_1 (all data)	0.0476	0.0311	0.0511
R_1	0.0420	0.0276	0.0365

(**6**, **9**, **10**, **12**, **21**) or Cu-K_α radiation (λ = 1.54178 Å) (**3**, **11**, **13**, **15**, **17**, **18**, **20**), a GV 50 diffractometer (Rigaku, formerly Agilent Technologies) with TitanS2 detector applying Cu–Kα radiation (λ = 1.54178 Å) (**1**, **4**, **5**) or Cu-K_β radiation (λ = 1.39222 Å) (**14**, **16**, **19**) or SuperNova (Agilent Technologies) with an Atlas detector applying Cu-K_α radiation (λ = 1.54178 Å) (**7**, **8**) or Mo radiation (λ = 0.71073 Å) (**2**). All measurements were performed at 123 K. Data collection and reduction were performed with CrysAlisPro[19] (Version V1.171.41.21a, 2019 (**11**), V1.171.40.14a, 2018 (**1**, **2**, **4**, **5**, **10**, **12**, **14**, **15**, **16**, **17**, **18**, **19**, **20**, **21**), V1.171.37.34, 2014 (**3**,**8**), V1.171.38.43, 2015 (**6**, **7**, **9**, **13**). A Gaussian absorption correction was performed using CrysAlisPro for **1**, **2**, **3**, **4**, **5**, **6**, **10**, **11**, **12**, **15**, **16**, **17**, **19**, **20**, **21**.[19] For **7**, **8**, **9**,**13**, 1**4**, **18** an analytical absorption correction was performed using CrysAlisPro using a multifaceted crystal model based on expressions derived by R.C. Clark & J.S. Reid.[20] Using Olex2,[21] all structures were solved by ShelXT.[22] A least-square refinement on F^2 was carried out with ShelXL.[23] All non-hydrogen atoms were refined anisotropically. Hydrogen atoms were located in idealized positions and refined isotropically according to riding model. Crystallographic data and structure refinement results are summarized in Table 1, Table 2, Table 3, and Table 4. Total energies (BP86/def2-TZVP level of theory) are listed in Table 5. Further crystallographic details are given in the Supporting Information.

Crystallographic data (excluding structure factors) for the structures in this paper have been deposited with the Cambridge Crystallographic Data Centre, CCDC, 12 Union Road, Cambridge CB21EZ, UK. Copies of the data can be obtained free of charge on quoting the depository numbers CCDC-2012897 (**1**), CCDC-2012898 (**2**), CCDC-2012899 (**3**), CCDC-2012900 (**4**), CCDC-2012901 (**5**), CCDC-2012902 (**6**), CCDC-2012903 (**7**), CCDC-2012904 (**8**), CCDC-2012905 (**9**), CCDC-2012906 (**10**), CCDC-2012907 (**11**), CCDC-2012908 (1**2**), CCDC-2012909 (**13**), CCDC-2012910 (**14**), CCDC-2012911 (**15**), CCDC-2012912 (**16**), CCDC-2012913 (**17**), CCDC-2012914 (**18**), CCDC-2012915 (**19**), CCDC-2012916 (**20**), and CCDC-2012917 (**21**) (Fax:

Table 5. Total energies (BP86/def2-TZVP level of theory).

	Total energy /Ha
10	–5970.84136015
11	–4477.13521401
12	–5062.20187374
13	–6262.04247322
14	–5510.36824102
15	–4149.50506370
16	–4005.45820135
17	–7958.63084809
18	–4352.52475218
19	–5529.81041966
20	–4036.10784837
21	–3892.06475106

+44-1223-336-033; E-Mail: deposit@ccdc.cam.ac.uk, http://www.ccdc.cam.ac.uk).

Computational Details: Gaussian 09 program[24] was used throughout. Density functional theory (DFT) in form of or BP86[25] (Becke's exchange and Perdew 86 correlation functional) with def2-TZVP all electron basis set was employed. For solvents effects has been accounted by using continuous polarizable continuum model (CPM).[26] The dielectric constant of dichloromethane (ε = 8.93) has been used in the calculations of the cations (**14**, **15**, **16**, **19**, **20**, **21**). The Natural Bond Orbital (NBO) analysis has been performed with the NBO6 program.[27] The dispersion correction GD3BJ was applied.[28] The figures for the supporting information concerning the DFT calculations were created with Chemcraft.[29] Atomic coordinates of **10**–**21** are given in the Supporting Information.

Supporting Information (see footnote on the first page of this article): Details of the X-ray structure analysis as well as of the computational details are given in the supporting information.

Acknowledgements

This work was supported by the Deutsche Forschungsgemeinschaft within the project Sche 384/38–1. MP is grateful to the Fonds der Chemischen Industrie for a PhD fellowship and to the DAAD for foundation during a research stay at Texas A&M University. FPG acknowledges support from the Welch Foundation (grant A-1423) and the National Science Foundation (grant CHE-1856453). Open access funding enabled and organized by Projekt DEAL.

Keywords: Bimetallic complexes; Metal–metal interaction; Tungsten; Coinage metal; Carbonyl ligands

References

[1] a) C. Silvestru, H. J. Breunig, H. Althaus, *Chem. Rev.* **1999**, *99*, 3277–3328; b) J. Burt, W. Levason, G. Reid, *Coord. Chem. Rev.* **2014**, *260*, 65–115; c) N. R. Champness, W. Levason, *Coord. Chem. Rev.* **1994**, *133*, 115–217.
[2] W. Levason, C. A. McAuliffe, *Acc. Chem. Res.* **1978**, *11*, 363–368.
[3] W. Levason, G. Reid, *Coord. Chem. Rev.* **2006**, *250*, 2565–2594.
[4] B. R. Higginson, C. A. McAuliffe, L. M. Venanzi, *Inorg. Chim. Acta* **1971**, *5*, 37–40.
[5] C. R. Wade, F. P. Gabbaï, *Angew. Chem. Int. Ed.* **2011**, *50*, 7369–7372.
[6] I.-S. Ke, F. P. Gabbaï, *Aust. J. Chem.* **2013**, *66*, 1281–1287.
[7] P. J. Fischer, A. P. Heerboth, Z. R. Herm, B. E. Kucera, *Organometallics* **2007**, *26*, 6669–6673.
[8] A. Blagg, A. T. Hutton, B. L. Shaw, M. Thornton-Pett, *Inorg. Chim. Acta* **1985**, *100*, L33-L34.
[9] B. Brumas-Soula, F. Dahan, R. Poilblanc, *New J. Chem.* **1998**, *22*, 1067–1074.
[10] J. T. Lin, Y. M. Hsiao, L. K. Liu, S. K. Yeh, *Organometallics* **1988**, *7*, 2065–2066.
[11] S. Alvarez, *Dalton Trans.* **2013**, *42*, 8617–8636.
[12] L. Carlton, W. E. Lindsell, K. J. McCullough, P. N. Preston, *J. Chem. Soc., Chem. Commun.* **1983**, 216–218.
[13] R. B. King, A. Fronzaglia, *Inorg. Chem.* **1966**, *5*, 1837–1846.
[14] A. Salzer, H. Werner, *Z. Anorg. Allg. Chem.* **1975**, *418*, 88–96.
[15] a) E. W. Abel, M. A. Bennett, G. Wilkinson, *Proc. Chem. Soc.* **1958**; b) E. W. Abel, M. A. Bennet, R. Burton, G. Wilkinson, *J. Chem. Soc.* **1958**, 4559; c) F. A. Cotton, J. A. Mccleverty, J. E. White, R. B. King, A. F. Fronzaglia, M. B. Bisnette, *Inorg. Synth.* **1990**, 45–47.
[16] C. R. Wade, I.-S. Ke, F. P. Gabbaï, *Angew. Chem. Int. Ed.* **2012**, *51*, 478–481.
[17] H. Yang, F. P. Gabbaï, *J. Am. Chem. Soc.* **2014**, *136*, 10866–10869.
[18] S. Ahrland, K. Dreisch, B. Norén, Å. Oskarsson, *Mater. Chem. Phys.* **1993**, *35*, 281–289.
[19] CrysAlis Software System, Rigaku Oxford Diffraction, **2018**.
[20] R. C. Clark, J. S. Reid, *Acta Crystallogr., Sect. A* **1995**, *51*, 887.
[21] O. V. Dolomanov, l. J. Bourhis, R. J. Gildea, J. A. K. Howard, H. Puschmann, *J. Appl. Crystallogr.* **2009**, *42*, 339.
[22] G. M. Sheldrick, *Acta Crystallogr., Sect. A* **2015**, *71*, 3.
[23] G. M. Sheldrick, *Acta Crystallogr., Sect. C* **2015**, *71*, 3.
[24] M. J. Frisch, G. W. Trucks, H. B. Schlegel, G. E. Scuseria, M. A. Robb, J. R. Cheeseman, G. Scalmani, V. Barone, B. Mennucci, G. A. Petersson, H. Nakatsuji, M. Caricato, X. Li, H. P. Hratchian, A. F. Izmaylov, J. Bloino, G. Zheng, J. L. Sonnenberg, M. Hada, M. Ehara, K. Toyota, R. Fukuda, J. Hasegawa, M. Ishida, T. Nakajima, Y. Honda, O. Kitao, H. Nakai, T. Vreven, J. A. Montgomery Jr., J. E. Peralta, F. Ogliaro, M. Bearpark, J. J. Heyd, E. Brothers, K. N. Kudin, V. N. Staroverov, T. Keith, R. Kobayashi, J. Normand, K. Raghavachari, A. Rendell, J. C. Burant, S. S. Iyengar, J. Tomasi, M. Cossi, N. Rega, J. M. Millam, M. Klene, J. E. Knox, J. B. Cross, V. Bakken, C. Adamo, J. Jaramillo, R. Gomperts, R. E. Stratmann, O. Yazyev, A. J. Austin, R. Cammi, C. Pomelli, J. W. Ochterski, R. L. Martin, K. Morokuma, V. G. Zakrzewski, G. A. Voth, P. Salvador, J. J. Dannenberg, S. Dapprich, A. D. Daniels, O. Farkas, J. B. Foresman, J. V. Ortiz, J. Cioslowski, and D. J. Fox, Gaussian, Inc., Wallingford CT, 2013.
[25] a) J. P. Perdew, *Phys. Rev. B* **1986**, 8822; b) A. D. Becke, *Phys. Rev. A* **1988**, 3098.
[26] a) J. Tomasi, B. Mennucci, R. Cammi, *Chem. Rev.* **2005**, *105*, 2999; b) G. Scalmani, M. J. Frisch, *J. Chem. Phys.* **2010**, *132*, 114110.
[27] NBO 6.0. E. D. Glendening, J. K. Badenhoop, A. E. Reed, J. E. Carpenter, J. A. Bohmann, C. M. Morales, C. R. Landis, F. Weinhold (Theoretical Chemistry Institute, University of Wisconsin, Madison, WI, **2013**), http://nbo6.chem.wisc.edu.
[28] a) S. Grimme, J. Antony, S. Ehrlich, H. Krieg, *J. Chem. Phys.* **2010**, *132*, 154104; b) S. Grimme, S. Ehrlich, L. Goerigk, *J. Comput. Chem.* **2011**, *32*, 1456.
[29] Chemcraft – Graphical Software for visualization of quantum chemistry computations. https://www.chemcraftprog.com.

Received: June 30, 2020
Published Online: Septemer 2, 2020